USGS-OFR-86-98

UNITED STATES DEPARTMENT OF THE INTERIOR

GEOLOGICAL SURVEY

POSTSHOT SEISMIC INVESTIGATIONS IN THE VICINITY OF THE MIDAS MYTH EVENT, U12t.04 DRIFT, NEVADA TEST SITE, NEVADA

By

R. D. Carroll and J. E. Magner

Open-File Report 86-98

Prepared in cooperation with the
Nevada Operations Office
U.S. Department of Energy
(Interagency Agreement DE-AI08-76DP00474)

and the
Defense Nuclear Agency

ILLUSTRATIONS--Continued

TABLES

POSTSHOT SEISMIC INVESTIGATIONS IN THE VICINITY OF THE MIDAS MYTH EVENT, U12t.04 DRIFT, NEVADA TEST SITE, NEVADA

By

R. D. Carroll and J. E. Magner

ABSTRACT

Seismic velocity investigations were undertaken in an attempt to help explain ground-shock damage that occurred in an underground recording alcove as a result of the Midas Myth nuclear explosion. Seismic velocity measurements conducted along refraction lines and in 12-m drill holes in the floor and back of the alcove reveal markedly lower velocities compared to undisturbed rock. The results can be explained qualitatively in terms of the velocity theory of Crampin (1978) for wet and dry fracture sets and suggest the existence of a biplanar fracture system parallel and normal to the alcove orientation. The parallel fracture set appears to be dry in the floor and back and is attributed to shock-induced bedding plane detachments. The normal fracture set is associated with faults in the area and appears to be saturated in the floor and drained in the back. Velocity decrease appears to be greatest in the vicinity of the faults. Refraction data indicate an enhancement of "dip" effects in the traveltime plots as a result of ground shock. Although the refraction data can be explained in terms of an apparent dipping low-velocity layer on the skin of the tunnel, it is felt that the results represent some as yet unmodelled fracture phenomenon resulting in detachments peculiar to the skin of the underground opening.

INTRODUCTION

The Midas Myth event was a low-yield nuclear event detonated in the U12t.04 drift in Aqueduct Mesa at the Nevada Test Site on February 15, 1984 (fig. 1). Reentry inspection of the tunnel showed that ground shock from the detonation had caused extensive collapse and damage to a recording alcove (known as the Ball Room) at a range of about 220 m from the detonation point. The reasons for some of this damage were of concern to the construction engineering staff of the Defense Nuclear Agency (DNA). One of several scenarios put forth to explain the phenomenon involved the possibility that fracture drainage from the back of the open tunnel coupled with saturation of fractures in the tunnel floor resulted in a differential shock-wave velocity producing an anomalously large upward acceleration component. At the request of the DNA, velocity measurements were undertaken in the vicinity of the Midas Myth reentry and in drill holes in the Ball Room in an attempt to determine to what extent the postshot environment exhibited seismic velocity anomalies. The velocity studies consisted of three phases:

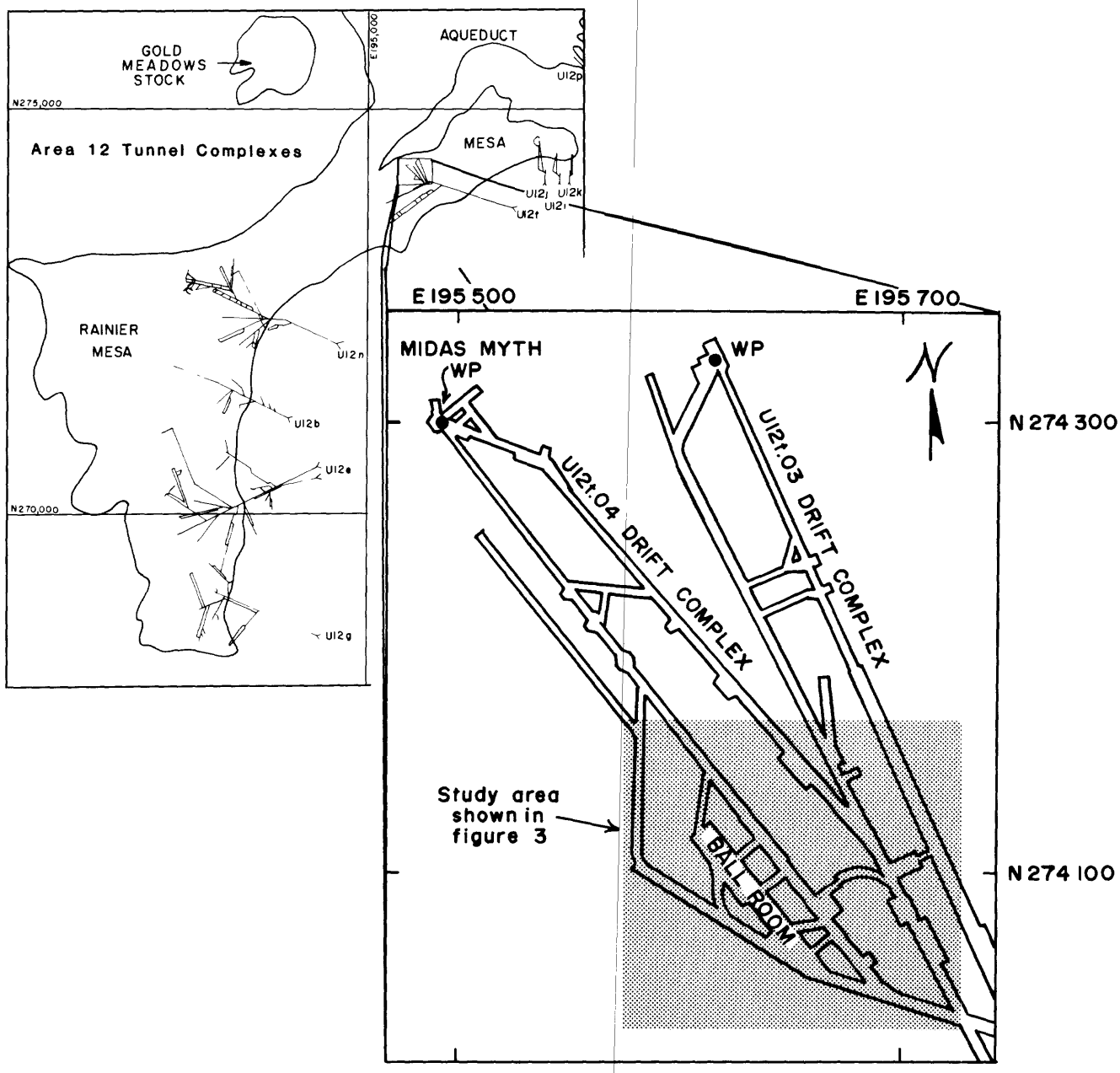

Figure 1.--Index map showing location of Midas Myth (U12t.04) drift complex.

1) Seismic refraction surveys in the floor and back of the reentry area. These data were obtained to evaluate if the more economical use of refraction surveys along the tunnel could yield an adequate velocity description without resorting to drill holes in any future applications of these techniques. An additional goal was to investigate the utility of refraction surveys in the back for long-term monitoring.
2) Inhole velocity surveys in 12-m drill holes in the floor and back.
3) Crosshole velocity surveys in the floor and back.

Geologic Setting

The Midas Myth (U12t.04) drift complex is located at a depth of 361 m beneath Aqueduct Mesa in Area 12 at the Nevada Test Site. The geology of the Aqueduct Mesa area has been mapped by Gibbons and others (1963) and Sargent and Orkild (1973). The geology of the tunnel level region consists of zeolitized ash-fall tuff and is well characterized by data from numerous vertical and horizontal drill holes in the area as well as by nearby drifts. A generalized geologic section of the Area 12 tunnel region is shown on figure 2. In the vicinity of the Midas Myth working point (WP), the zeolitization of the tuff extends from below the tunnel to about 97 m above the tunnel where, except for a thin, welded ash-flow unit at about 151 m above the tunnel, vitric ash-fall tuff comprises the section to the base of the welded tuff capping the surface of the mesa. The welded cap is about 113 m thick. Beneath the tunnel site, ash-flow and ash-fall tuffs comprise the section to a depth of 314 m where pre-Tertiary rocks consisting chiefly of quartzite and dolomite are encountered. A thin, densely welded tuff is also present about 58 m below the tunnel. The geologic structure in the area of the tunnel consists of north- to northeast-trending normal faults with displacements not exceeding a few meters. The geologic structure in the underground area where seismic data were gathered in this investigation is shown on figure 3. A syncline is present in the tunnel in this region and the beds are marked by essentially flat dip near the axis with dips of 6 to 15° on the limbs. The tunnel environment can be further characterized by the following physical properties in the vicinity of the WP:

Overburden density	1.8 Mg/m^3
Bulk density	1.9 Mg/m^3
Compressional velocity	2.6 km/s
Water content (wt percent)	21
Porosity (percent vol)	40
Saturation (percent)	97

As the velocity of the tuff is the property of prime interest in this investigation, the seismic refraction data obtained in the t.04 drift prior to detonation of the Midas Myth event are shown on figure 4. The locations where these measurements were taken are shown on figure 3.

Acknowledgments

The impetus for this study was provided by J. W. LaComb, DNA. The geologic mapping in the measurement region was done by Fenix & Scisson, Inc.

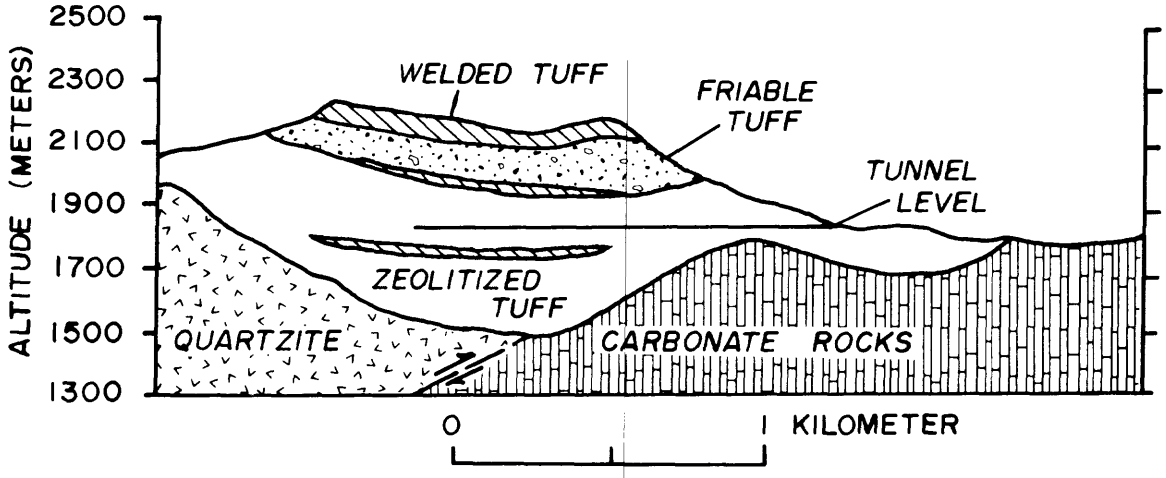

Figure 2.--Generalized geologic cross section through Rainier and Aqueduct Mesa tunnel area.

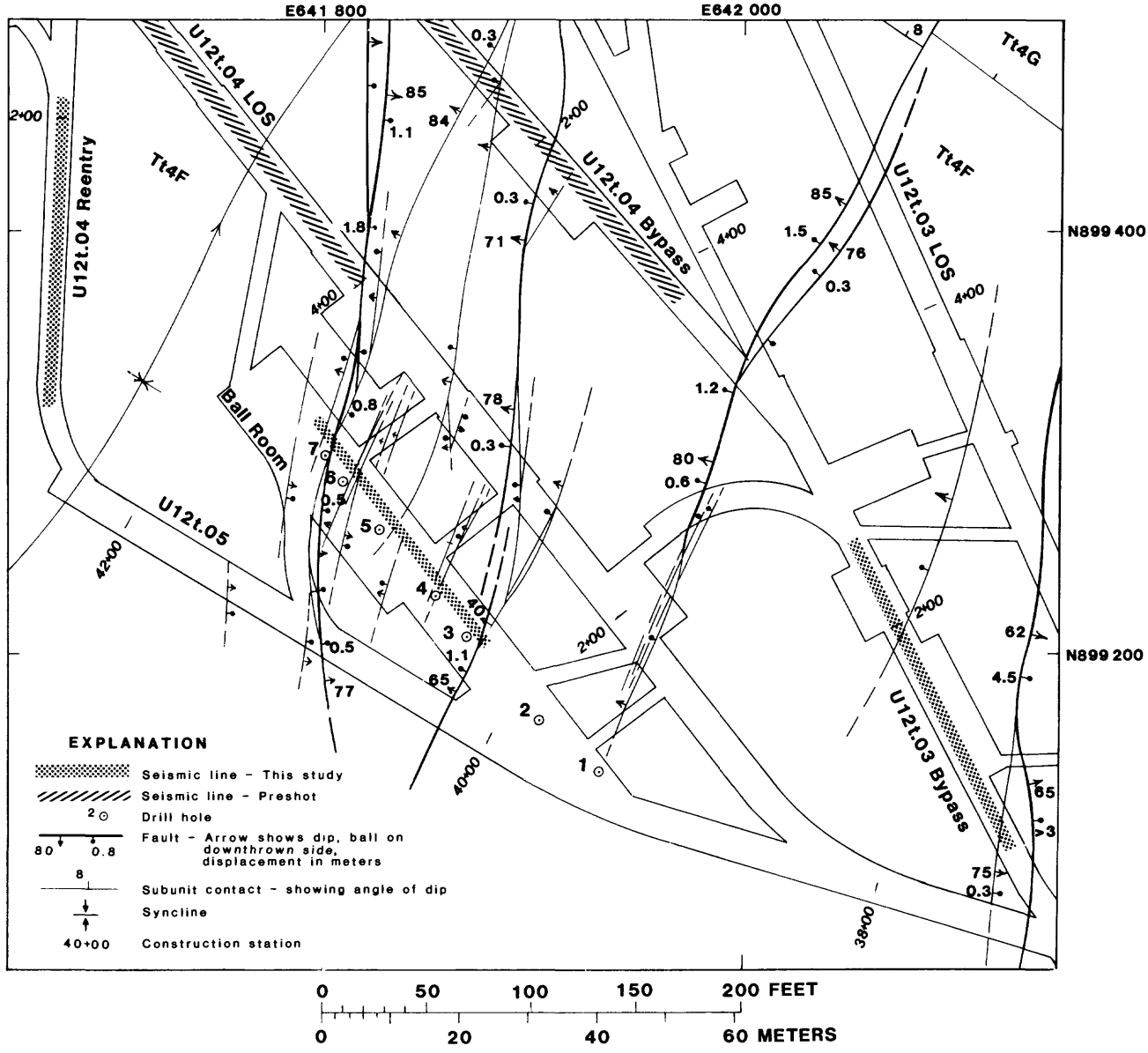

Figure 3.--Portion of U12t.04 reentry area showing locations of seismic lines and drill holes where seismic measurements were made (Geology mapped by Fenix & Scisson Inc.).

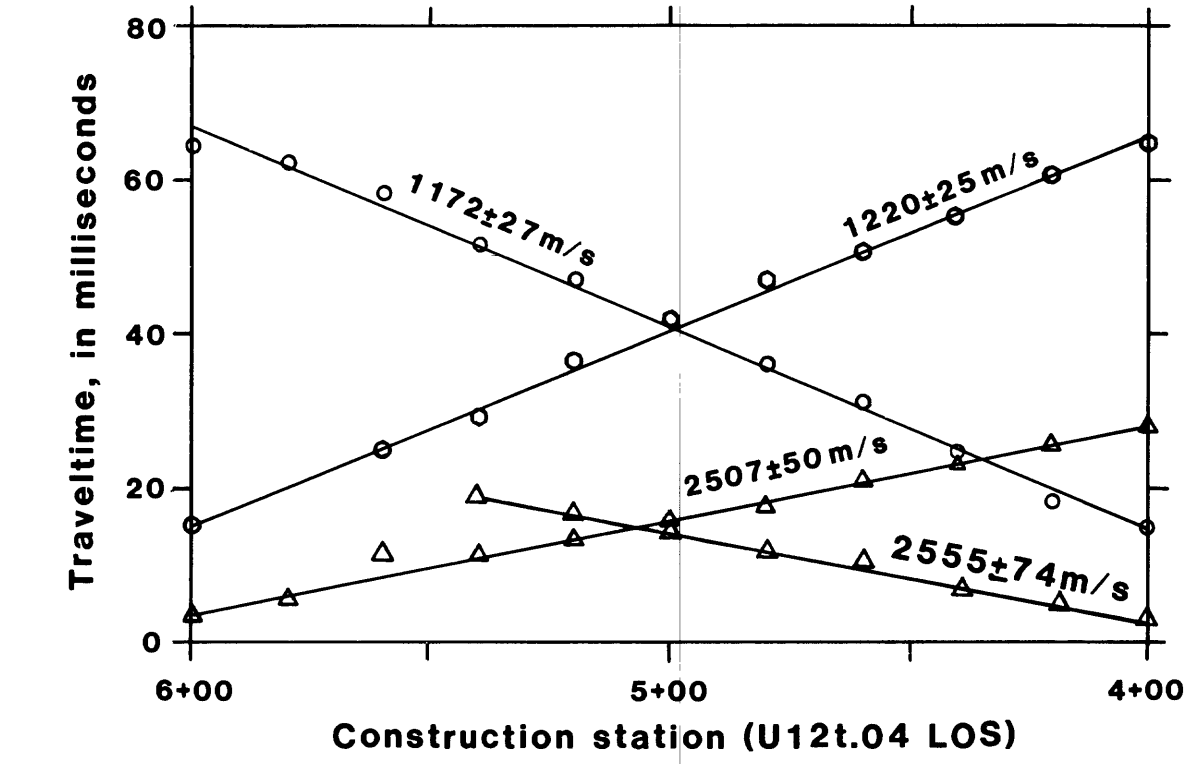

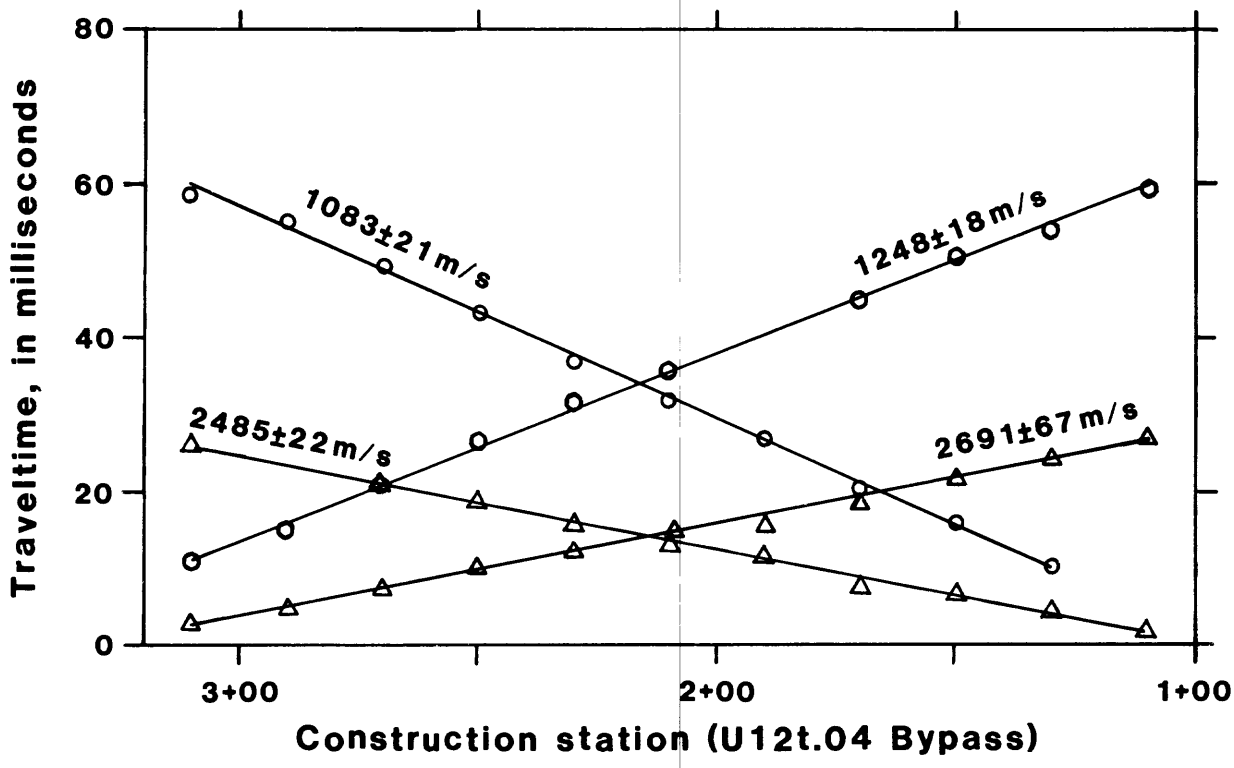

Figure 4.--Seismic refraction results obtained in vicinity of the Ball Room prior to Midas Myth detonation (○= S-wave arrival time, △= P-wave arrival time).

RELATIONSHIP OF VELOCITY TO FRACTURES

Both interstitial and fracture porosity and the relative amounts of air and water within the pore space of a rock are known to affect both shear- and compressional-wave velocities in geologic media. Only relatively recently, however, have attempts been made to quantitatively derive expressions for the effects of the relative proportions of gas and liquid in the pore space on the propagation velocity of seismic waves. In the case of the connected porosity, exclusive of fractures, the "bright spot" criteria in petroleum exploration has led to fair quantitative approximations describing the effect of water saturation on the compressional- and shear-wave velocities (Domenico, 1974, 1976). The more formidable problem of describing the effect of the wet and dry states of fractures on velocities has also received theoretical treatment. O'Connell and Budiansky (1974) have theoretically treated the effect of randomly oriented fractures on the shear- and compressional-wave velocities, and used their results to describe observed velocity variations in connection with earthquake precursors. Crampin (1978) and Crampin and others (1980) have derived theoretical relationships for the effect of oriented crack systems on P- and S-wave velocities. These relationships are of utility in performing velocity measurements across cracks in that they enable estimates to be made of the effect of the relative orientation of cracks (dry or saturated) and the direction of wave propagation on observed shear- and compressional-wave velocities. For a system of dry cracks these relationships are (Crampin and others, 1980):

$$V_p = V_{p_o} \Big/ \left(1 + \frac{8}{3}\,\varepsilon \left\{\frac{8}{7}\,(c^2 - c^4) + [(1 + 2c^2)^2/4]\right\}\right)^{1/2},$$

and (1)

$$V_s = V_{s_o} \Big/ \left(1 + 16\varepsilon \left\{\frac{c^2 \cos^2\phi}{7} + \frac{(1 - 2c^2)^2}{7} \sin^2\phi + \left[\frac{(c^2 - c^4)}{4} \sin^2 \phi\right]\right\}\right)^{1/2}$$

where

V_{p_o} and V_{s_o} are the compressional- and shear-wave velocities of the uncracked solid

$\varepsilon = Na^3/v$, the crack density of N cracks of radius a in volume v,

c = cosine of the angle of incidence of propagation to the parallel cracks,

ϕ = angle of polarization of the shear wave to the normal of the plane of incidence (90° for SH, 0° for SV).

Figure 5a clarifies the geometry implied in equation 1 with respect to the shear-wave polarizations and the tunnel orientation. The azimuthal reference is the relationship of the P wave, measured in its plane of incidence, to the fracture plane. This is 0° for the configuration shown on figure 5a (P wave normal to the fracture plane). The shear modes, SH and SV, are orthogonal and lie within a plane perpendicular to the P-wave plane of incidence. The SH polarization may also be considered to lie within the plane of incidence with the SV polarization perpendicular to the incidence plane. The addition of a second fracture set to form a biplanar system at angle is also shown.

The geometry depicted is for vertical fracture systems but can easily be applied to fractures of any orientation if one keeps in mind that the SV mode is defined as always parallel to the fracture planes of interest and not necessarily polarized in the vertical (gravity) direction. Thus, some care must be exercised in defining the SV and SH modes. An example is shown on figure 5b. Here we are interested in applying equation 1 to determine the relative effect of a single fracture system, horizontal and parallel to the tunnel, on the three velocities. (This is represented in a real sense in the Rainier Mesa tunnels by the bedding plane attitude of the tuff with respect to the tunnel.) The configuration on figure 5b is obtained by rotating the P-wave vector on figure 5a 90°, and noting that the "SH" mode calculated from equation 1 is the only mode "sampling" the fracture. We have redrawn the tunnel to show its true configuration with respect to the fracture system for this geometry. Note that one would normally call the SH polarization shown on figure 5b the SV mode because with respect to the tunnel that is the vertical (gravity) direction.

Fortunately we will be able to avoid such subtleties in discussing the geometries used in this investigation. It should be kept in mind, however, that when measuring velocities over different travel paths with respect to fracture sets as was done in this investigation (e.g., along tunnels versus along drill holes perpendicular to the tunnel) the definition of the shear mode polarizations are important when velocity comparisons derived from equation 1 are employed.

The terms in brackets in equation 1 are omitted to obtain the velocity variation for a system of wet cracks. The cracks defined by Crampin are penny shaped, a crack density of ε=0.1, for example, being equivalent to a 9-mm-diameter crack in each cubic centimeter of volume of material traversed by the wavefront. For an assumed crack density of this magnitude and typical unfractured tuff velocities--a shear wave velocity of 1300 m/s (Poisson's ratio of 1/3) and a compressional velocity of 2600 m/s--the velocities of the P, SH, and SV modes of propagation as a function of the orientation of the fracture system to the seismic line (direction of the tunnel) may be calculated by equation 1. Selecting an arbitrary crack density of 0.1 the results are shown on figure 6. The reductions in velocity as a decimal percent of the velocity of the uncracked material are listed in table 1 for angles of incidence of 5° in the range 0° (P-wave propagation perpendicular to crack system) to 90° (P-wave propagation parallel to the crack system). Obvious limitations exist on the strict use of these equations with regard to the reality of the magnitude of fracture density required to get significant velocity changes such as were observed in this investigation, and the applicability of penny-shaped cracks to other than microfailed systems.

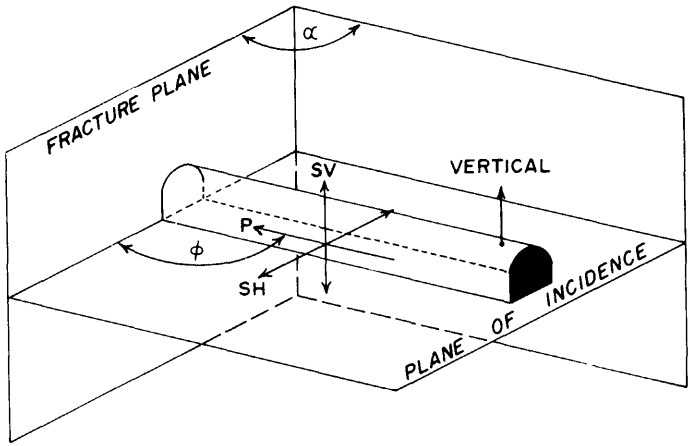

a. Geometry for single or biplanar fracture system, $\phi = 0°$, $\alpha = 90°$

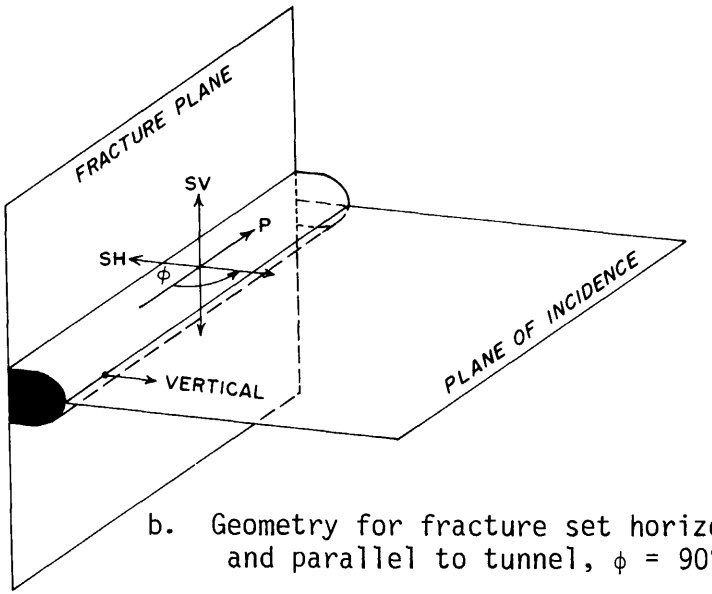

b. Geometry for fracture set horizontal and parallel to tunnel, $\phi = 90°$

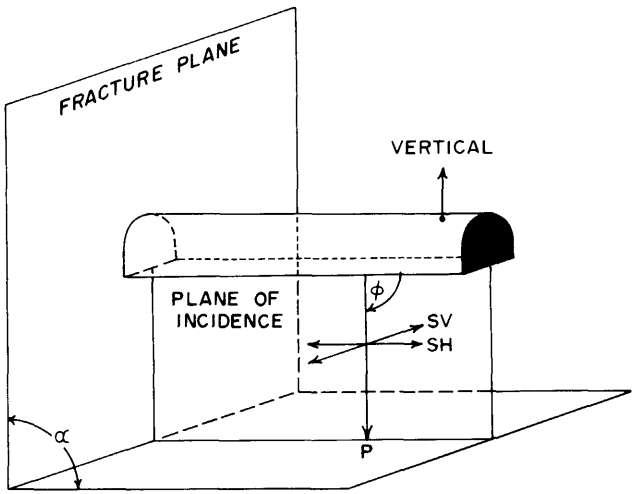

c. Geometry for inhole velocity measurements, $\phi = 0°$, $\alpha = 90°$

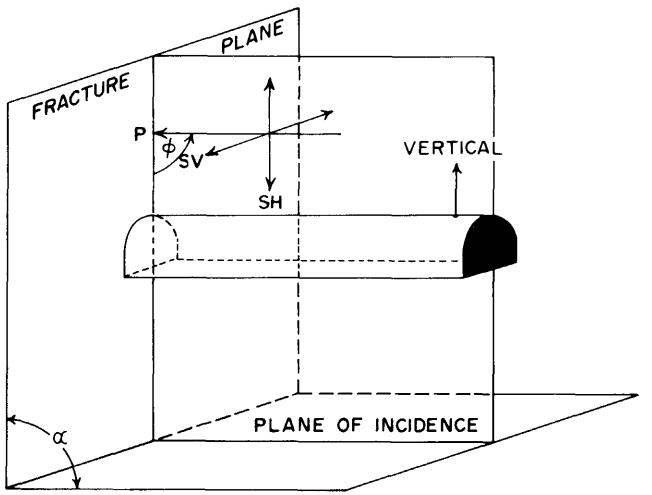

d. Geometry for crosshole velocity measurements between holes in back or floor, $\phi = 0°$, $\alpha = 90°$

Figure 5.--Relationships between propagation modes derived from Crampin's equations and various measurement configurations.

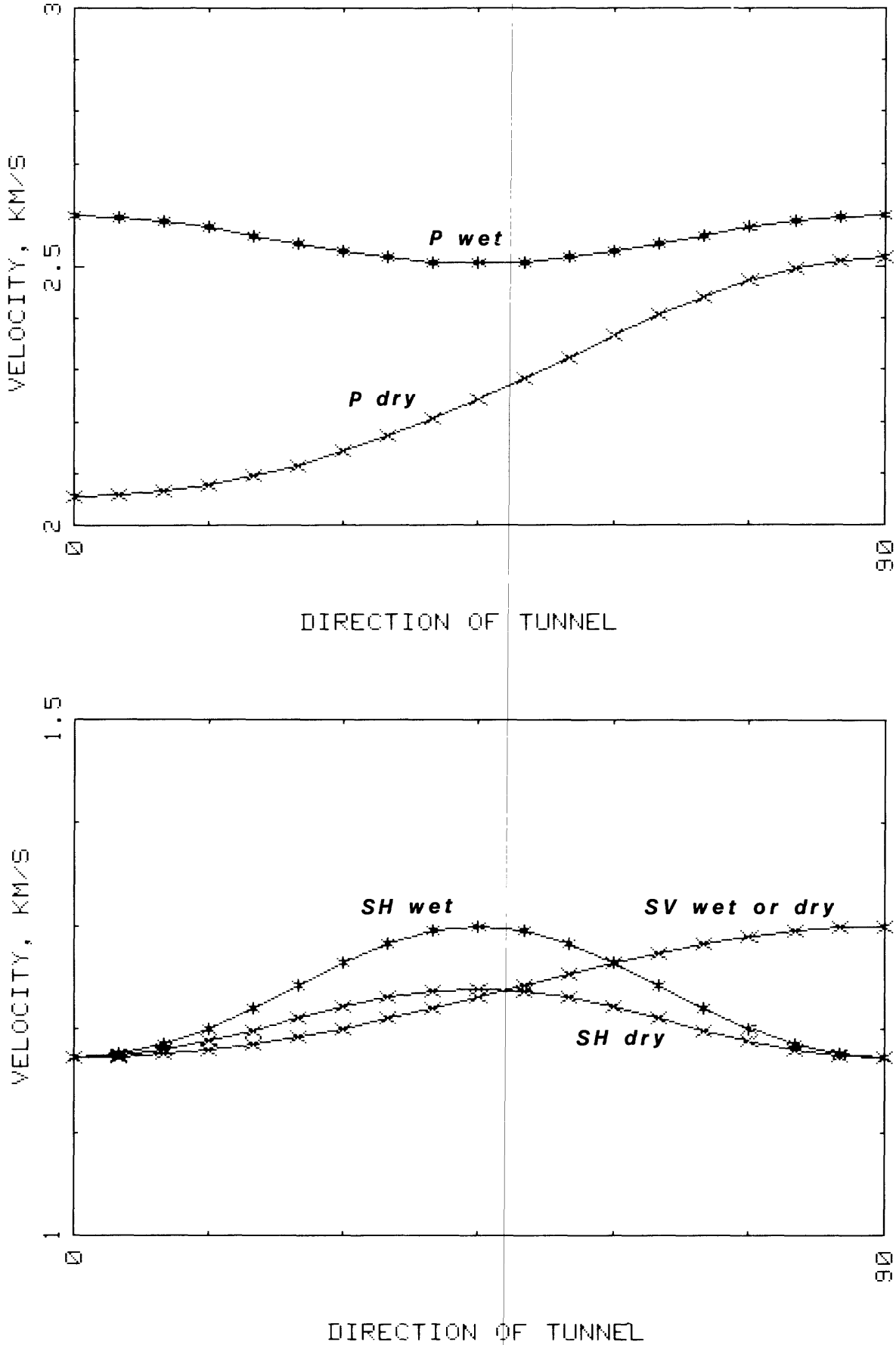

Figure 6.--Theoretical P- and S-wave velocities obtained along a tunnel for a wet and dry vertical fracture system at various orientations to the tunnel. 0 direction is for tunnel normal to fracture system.

Table 1.--Normalized values of theoretical P- and S-wave velocity calculated for 5 degree azimuths to a vertical, wet- and dry-fracture system.

Azimuth	P		SH		SV
	(dry)	(wet)	(dry)	(wet)	(dry or wet)
0 [1]	0.791	1.000	0.902	0.902	0.902
5	0.792	0.999	0.904	0.905	0.903
10	0.794	0.996	0.908	0.912	0.905
15	0.799	0.991	0.914	0.924	0.908
20	0.805	0.985	0.922	0.939	0.912
25	0.814	0.978	0.931	0.956	0.918
30	0.824	0.973	0.940	0.973	0.924
35	0.835	0.968	0.947	0.987	0.931
40	0.849	0.965	0.952	0.997	0.939
45	0.863	0.964	0.953	1.000	0.947
50	0.878	0.965	0.952	0.997	0.956
55	0.894	0.968	0.947	0.987	0.964
60	0.910	0.973	0.940	0.973	0.973
65	0.925	0.978	0.931	0.956	0.980
70	0.939	0.985	0.922	0.939	0.987
75	0.951	0.991	0.914	0.924	0.992
80	0.961	0.996	0.908	0.912	0.997
85	0.966	0.999	0.904	0.905	0.999
90	0.968	1.000	0.902	0.902	1.000

[1] Tunnel normal to fracture system at 0 degrees

However, the relationships are of considerable value in allowing estimates to be made of the effects on velocity of the relative orientation of the fractures and the direction of wave propagation. In addition, knowledge of the relative ability of the three wave types to reflect fractures on the basis of velocity changes with regard to both direction and saturation is of importance in planning and evaluating the results of measurements. These points assume greater significance when measurement locations are limited as is the case in a tunnel. Applications of these equations in explaining field observations have been reported (Crampin and others, 1980; Leary and Henyey, 1985).

A number of interesting conclusions can be drawn from figure 6, the most notable being that for this model the saturated crack system has no effect upon the magnitude of the compressional velocity at either normal or tangential orientations and an insignificant effect (4 percent reduction at maximum) at all orientations of the tunnel (seismic line) to the fracture system. The dry system on the other hand exhibits a maximum effect on the compressional velocity at normal incidence to the fracture system (a 21 percent reduction in this case) and a trivial effect at tangential incidence (a 4 percent reduction in the velocity). Note that in this model if the tunnel were oriented subparallel to the fracture system, no significant compressional or SV velocity difference is predicted for the two saturation states. The SV mode exhibits the same velocity whether the rock is wet or dry and at tangential incidence propagates at the unfractured velocity. Given the direction of particle motion, this behavior of the P and SV velocities for propagation tangential to the fracture system is intuitively expected. The SH mode exhibits maximum velocity decrease (in this case a 10 percent velocity reduction) at both normal and tangential orientations. The SV mode exhibits the same reduction at normal incidence only. The SH mode propagates at only a slightly lower velocity (5 percent) at oblique incidence for a dry system of fractures than it does for a wet system. The SH mode propagates with no velocity reduction for 45° incidence to a saturated system.

When one considers the possibility of defining differences in velocity due to wet and dry states of fractures in the back and floor of a tunnel arising from the essentially vertical fracture (fault) system shown on figure 3, the above data may be summarized as follows:

a) The best velocity sensitivity to fracturing for measurements along a tunnel lies in the measurement of the compressional velocity when the fracture system is near perpendicular to the seismic line (tunnel) orientation.
b) Based on observed differences in velocity the SV mode is not suggested by these equations to yield any velocity difference to these two states regardless of orientation of the system.
c) Only at oblique incidence is the SH mode sensitive to the two saturation states; however, the compressional velocity is indicated to be more sensitive at normal incidence to the two saturation states than are the shear modes at all orientations.

The Ball Room, in which the majority of the measurements in this investigation were made, was subjected to heave of the floor along the fault plane in the vicinity of hole 7 (fig. 3). In addition, the floor and the back were probably subjected to bedding plane separation subparallel to the

tunnel. This bedding plane separation produced a second set of fractures resulting in the formation of a biplanar crack system in which the fractures due to the fault system are at approximately right angles to the parting along the bedding. In this instance equation 1 is modified by multiplication by a second term involving the angle of intersection of the set of cracks (Crampin and others, 1980, p. 349, eqs. 7-9). Using the same arbitrary crack density and a biplanar system at 90°, the resulting velocity variations with azimuth would be as shown on figure 7. The reductions in the velocity of the uncracked solid for the different propagation modes for this case are listed in table 2.

Again it is important to clarify the geometry of the fracture system and the measurement configuration with reference to wave polarization. Figure 5a is the geometry for which the data on figure 7 apply. In our investigations, measurements were made both along and between holes in the floor and back of the tunnel. The relationships between these measurement configurations, figure 5a, and the data on figure 7 are shown on figures 5c and 5d. Reflection on the geometries shown on figure 5 will indicate that considerations of polarization geometry are least confusing for the case of the P-wave velocity. The compressional velocity is the mode upon which our conclusions in this study were based; however, it is important to remember the relativity of the SH and SV polarization direction in the geometry of the investigation.

The data on figure 7 indicate that:

a) The compressional velocity is again most sensitive to the saturation state of the fractures. The addition of an orthogonal set of fractures now renders the model sensitive to differences between the wet- and dry-compressional velocity for all orientations of the tunnel/fracture system.
b) Differences in the the SV velocity are again insensitive to the two saturation states. Assuming one has a knowledge of the unfractured velocity, the low velocity of propagation of the SH and SV modes at normal or tangential incidence, however, may be of utility in defining the presence of fractures but not the saturation state.
c) Differences in the propagation velocity of the SH mode are of utility in defining the two saturation states near 45° incidence of the tunnel to the fracture system.

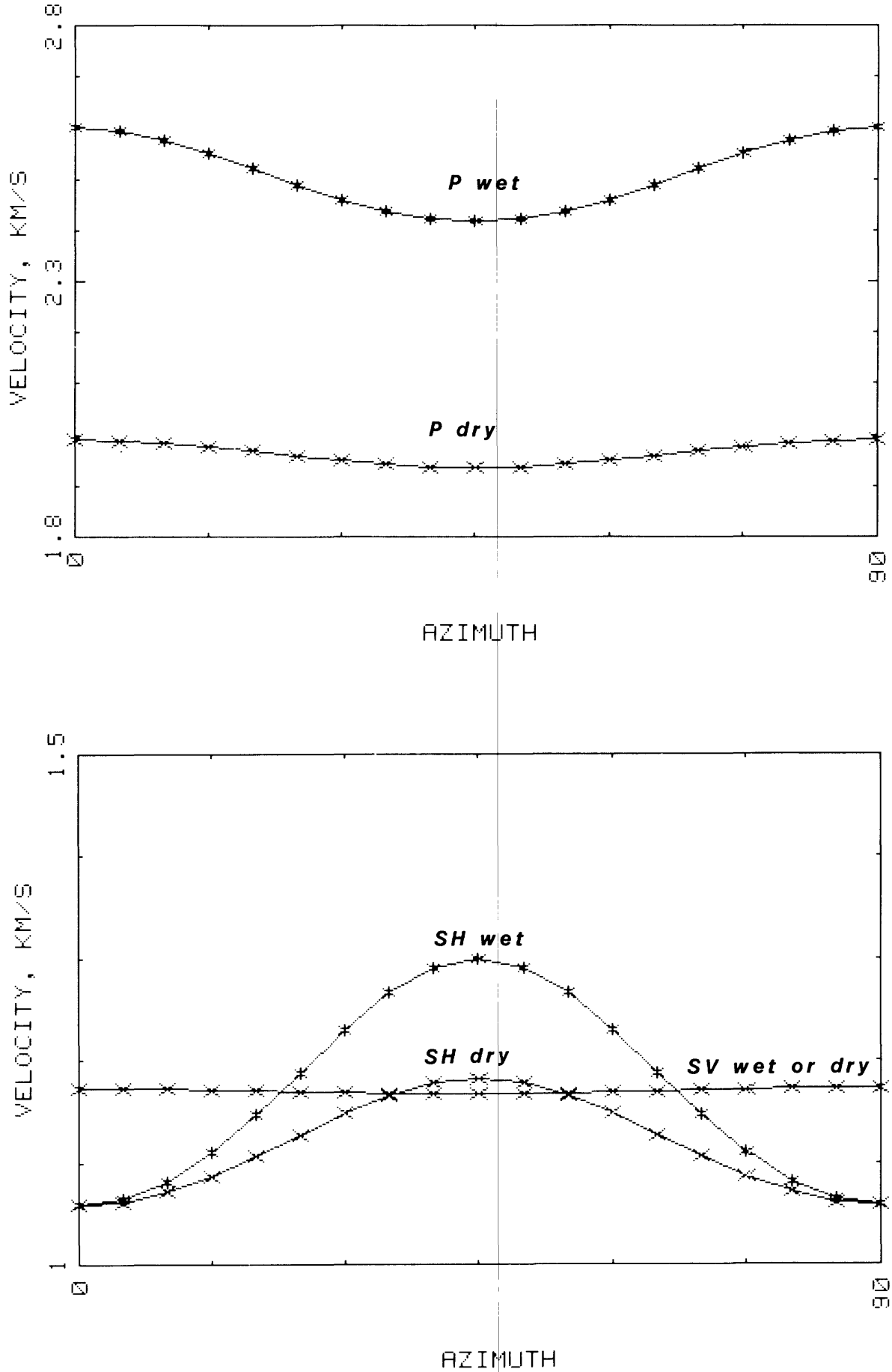

Figure 7.--Theoretical P- and S-wave velocities obtained along a tunnel for a biplanar (90°) vertical set of wet and dry fractures at various orientations to the tunnel.

Table 2.--Normalized values of theoretical P- and S-wave velocity calculated for 5 degree azimuths to a vertical, biplanar (90 degree), wet- and dry-fracture system

Azimuth	P		SH		SV
	(dry)	(wet)	(dry)	(wet)	(dry or wet)
0	0.765	1.000	0.814	0.814	0.902
5	0.765	0.998	0.817	0.819	0.902
10	0.763	0.991	0.824	0.832	0.902
15	0.760	0.981	0.836	0.854	0.901
20	0.757	0.969	0.851	0.882	0.900
25	0.753	0.957	0.867	0.914	0.899
30	0.750	0.946	0.883	0.946	0.899
35	0.747	0.937	0.897	0.974	0.898
40	0.745	0.931	0.906	0.993	0.898
45	0.745	0.929	0.909	1.000	0.897
50	0.745	0.931	0.906	0.993	0.898
55	0.747	0.937	0.897	0.974	0.898
60	0.750	0.946	0.883	0.946	0.899
65	0.753	0.957	0.867	0.914	0.899
70	0.757	0.969	0.851	0.882	0.900
75	0.760	0.981	0.836	0.854	0.901
80	0.763	0.991	0.824	0.832	0.902
85	0.765	0.998	0.817	0.819	0.902
90	0.765	1.000	0.814	0.814	0.902

The foregoing yield some idea of the velocity variations to be anticipated for a given fracture environment and tunnel orientation.[1] An examination of figure 3 suggests that as a first approximation the fractures associated with the fault system in the Ball Room strike nearly normal to the measurement line and close to the optimum configuration for the use of differences in compressional velocity measurements to define a wet and dry fracture system in the floor and back of the tunnel. Attempts were made in the course of this investigation to record the shear mode by the use of vertical and transverse geophones. Unfortunately shear waves were rarely recognized.

SEISMIC REFRACTION MEASUREMENTS ALONG THE BACK AND FLOOR

Postshot measurements of compressional velocity were made at the three locations shown on figure 3. The t.04 reentry drift was mined immediately after the Midas Myth detonation and represents a freshly mined tunnel of relatively small diameter. The Ball Room, the location of paramount interest, was mined as part of the Midas Myth complex in 1983, and the t.03 bypass drift was mined in 1975 as part of the Husky Pup experiment detonated that year. The seismic refraction surveys run nearest to the Ball Room prior to the Midas Myth detonation are located on figure 3, and the data are reproduced on figure 4. These data may be considered representative of velocity of tuff in the area prior to the Midas Myth detonation.

Geophone stations along each of the three lines were laid out along the floor and back on 4.6 m centers. In the Ball Room, the presence of a layer of concrete in the floor, several feet thick in places, negated the use of the refraction technique at that location. A standard set of refraction geophones was used in the floor with the sensors planted in holes in the tuff. In the back geophone inserts (Mark Products type L-21A) were used without the protective case. This insert has a sufficiently stiff suspension element to be utilized in the horizontal or vertical mode, although the method eventually used in planting the geophone utilized the normal vertical position. The geophone inserts were housed in 1.9-cm ID PVC tubing with the inner diameter of the end opposite the geophone tapped. The tubing was screwed onto the end

---

[1]These data yield insight into one of the possible reasons the shear velocity is diagnostic (in that it yields values below the experience histogram for virgin tuff) with regard to shock damage of tuff in the microfailed region close in to nuclear explosions, whereas decreases in the compressional velocity are less noticeable (Carroll, 1983). This is predicted to some extent by Crampin's theory if the microfractures are saturated. Similar relative decreases in the compressional and shear velocity are predicted for a random orientation of saturated fractures by O'Connell and Budiansky (1974), a model probably more applicable to the microfailed zone near explosions.

Figure 5b also suggests an explanation for the low shear velocity frequently observed in the region beyond the microfailed region surrounding nuclear explosions in tuff. P-wave velocity changes in this zone are often not noteworthy. The shear-wave polarization used in tunnel measurements is vertical to the tunnel and thus would "sample" bedding plane detachments which are essentially horizontal as depicted on figure 5b. The P-wave velocity would be less affected by such detachments.

of a 1.9-cm-diameter solid PVC rod after the rod had been grouted into 2.5-cm-diameter holes drilled with an electric drill 0.2 to 0.3 m into the back of the tunnel. The takeout positions of a standard 12-channel geophone cable were hung from wire mesh or rockbolts, and connections made from the takeouts to the geophones via a 1.2-m cable containing a standard split-plug connection on one end and a female Cannon plug on the other.

Plug tips soldered to leads were inserted in the Cannon plug with the opposite ends soldered to the geophone inserts. The wires were run from the geophones through a hole drilled into the side of the tubing housing the geophones. Details of these arrangements are shown on figure 8. The recording system was a Geometrics 1210F refraction unit.

Energy sources for these surveys consisted of caps and a few centimeters of detonating cord placed about 0.3-0.4 m deep in 2.5-cm-diameter holes drilled into the back and floor of the drift.

The results of the refraction surveys at the three locations shown on figure 3 are presented on figures 9-11. Two general observations are in order about these results: First, the velocity data all exhibit two-way differences suggesting geologic dip (apparent lower velocity) prevailing in the direction away from the WP; Second, the velocities in the freshly mined t.04 reentry drift (fig. 10) are not significantly different from the preshot velocity measured in the area (fig. 4).

The U12t.03 Drift

The results of the postshot (nuclear detonation) surveys in the t.03 drift may be interpreted in terms of a simple, dipping layer as shown on figure 12. A comparison of these data with the surveys obtained prior to the nuclear detonation in the region (fig. 4) as well as with the preshot data base for the Rainier Mesa area (Carroll and Kibler, 1983) indicates that even the second layer velocities (2007-2112 m/s) are too low for general experience in undisturbed tuff. Given the depth of investigation limitations imposed by the seismic spread length, an undisturbed velocity of 2600 m/s would require a minimum depth of about 7-8 m of degraded tuff surrounding the tunnel surface to yield the results depicted.

In connection with these results it should be noted that the general preshot experience in the tuff indicates little if any effects of dip. The tunnel beds generally vary in dip from 0 to over 16° in the areas where we have refraction experience; however, no survey indicates a consistent difference in two-way velocities on all lines in the direction one would expect from dips mapped locally. In the preshot data for which velocity differences might be attributable to dip, the magnitude of the velocity differences is considerably less (less than 10 percent) than those seen in the t.03 data. Furthermore, there is no evidence in the preshot experience of the development of any thickness of a surface layer as there is no velocity segment developed for this layer on the traveltime plot. In this respect, the results in the t.04 drift (fig. 10) are typical. This means that either the surface layer is of a nature that it would only be evident on a traveltime plot containing data points between the shotpoint and the first detector, or the difference in velocity between the two layers is of such a small magnitude (less than 5 percent) that we cannot discriminate between them on the

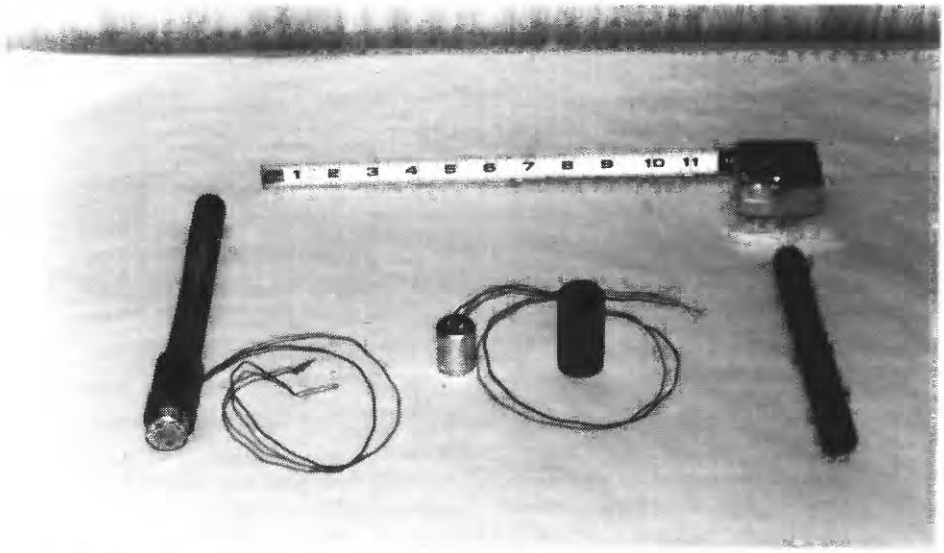

a)

b)

Figure 8.--Details of geophone assembly used in refraction survey in the back. a) Left to right: complete assembly; geophone insert and housing; PVC rod with threaded end for housing, opposite end is grouted in back. b) Assembly grouted in back and connected to geophone cable.

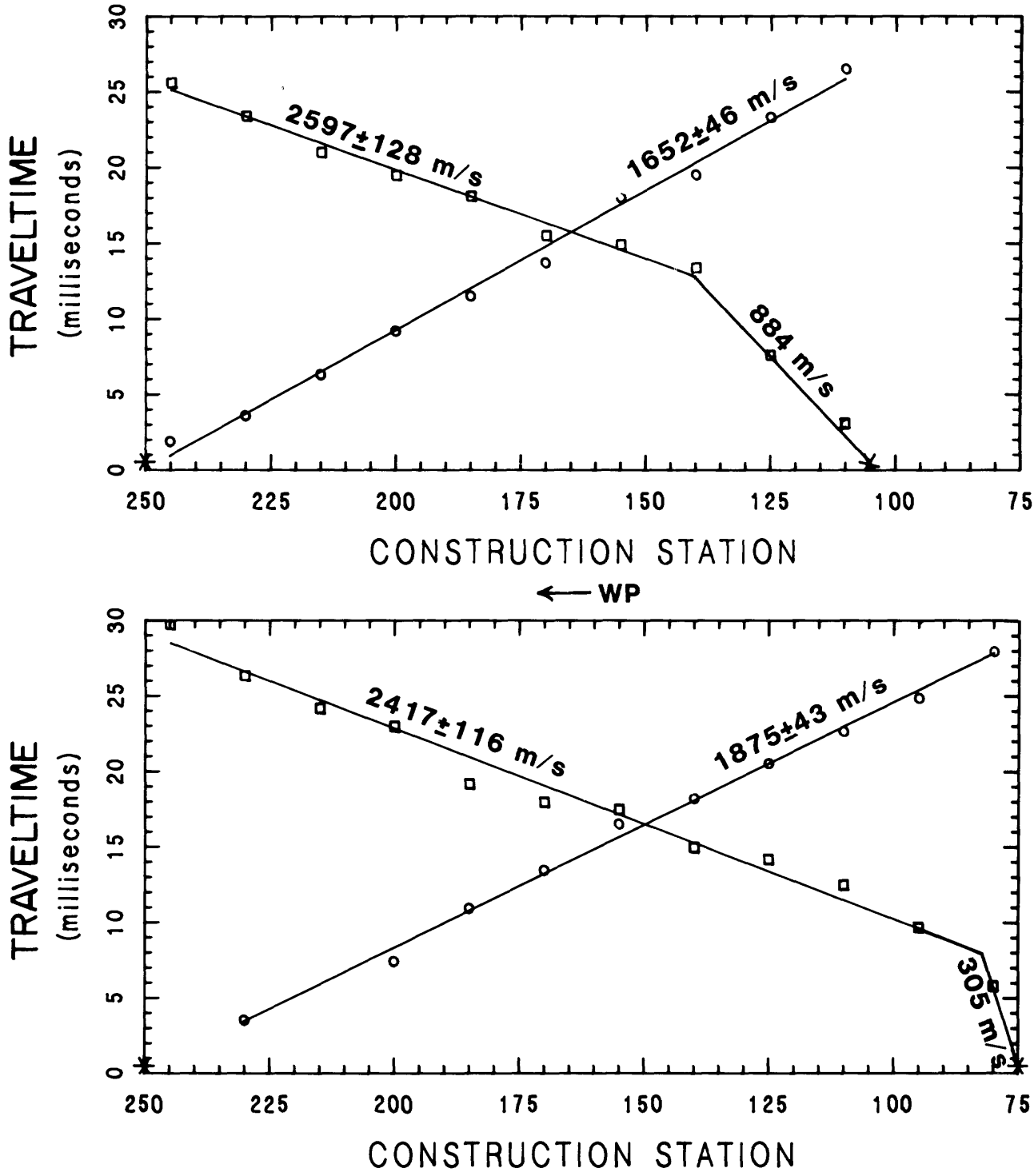

Figure 9.--Results of seismic refraction measurements in the back (top) and floor (bottom) of the U12t.03 bypass drift ("*" denotes shotpoint).

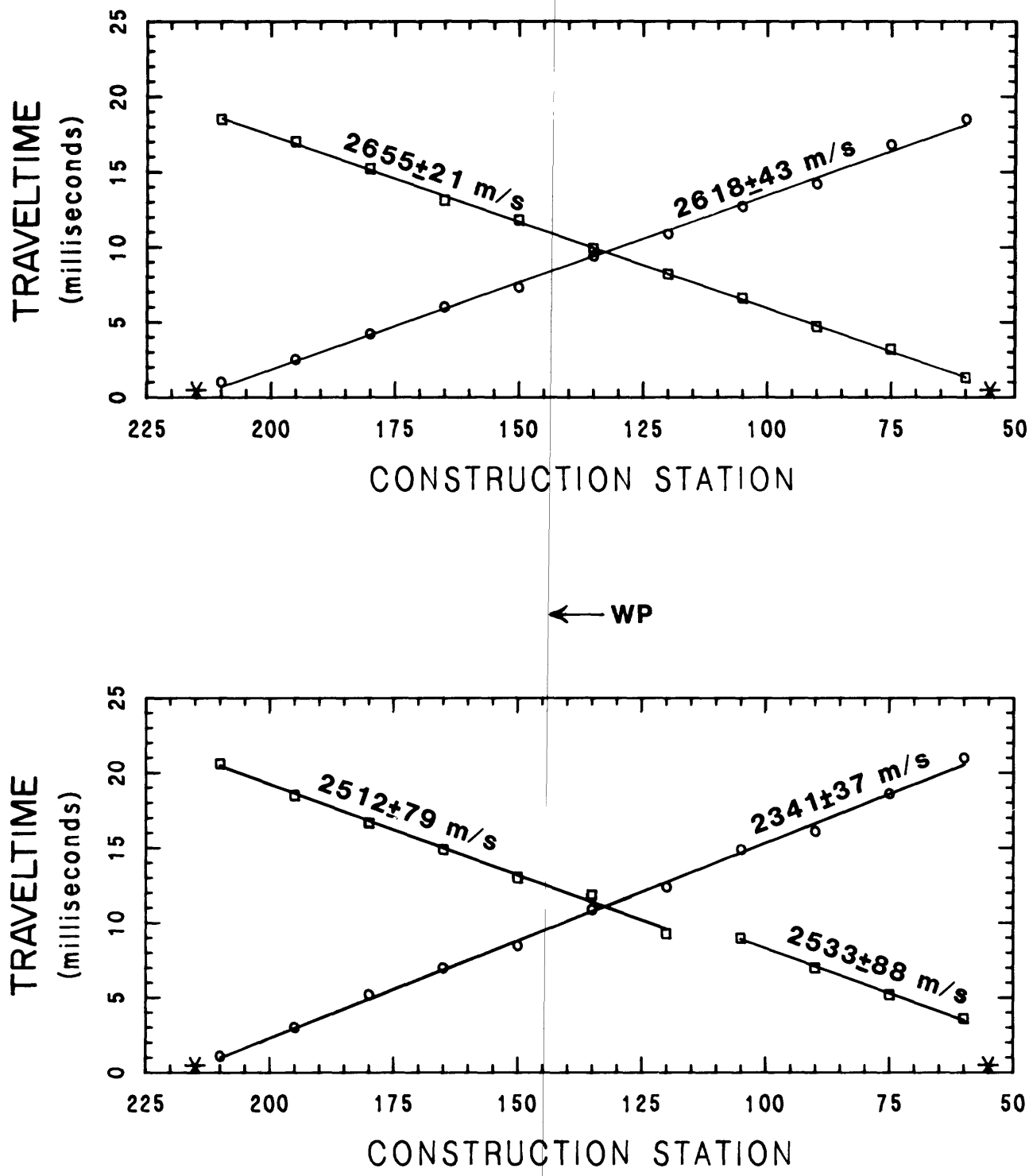

Figure 10.--Results of seismic refraction measurements in the back (top) and floor (bottom) of the U12t.04 reentry drift ("*" denotes shotpoint).

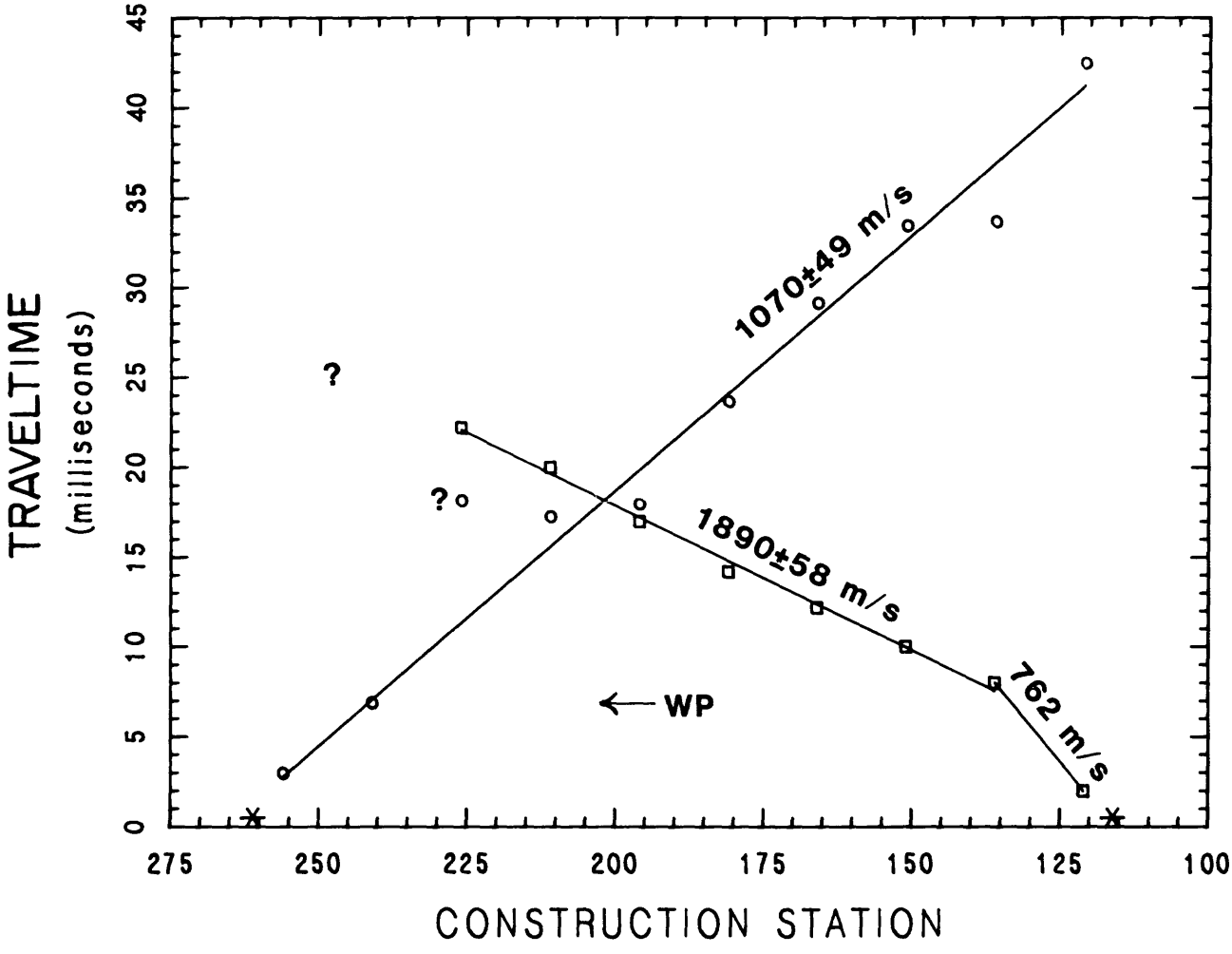

Figure 11.--Results of seismic refraction measurements in the back of the Ball Room ("*" denotes shotpoint).

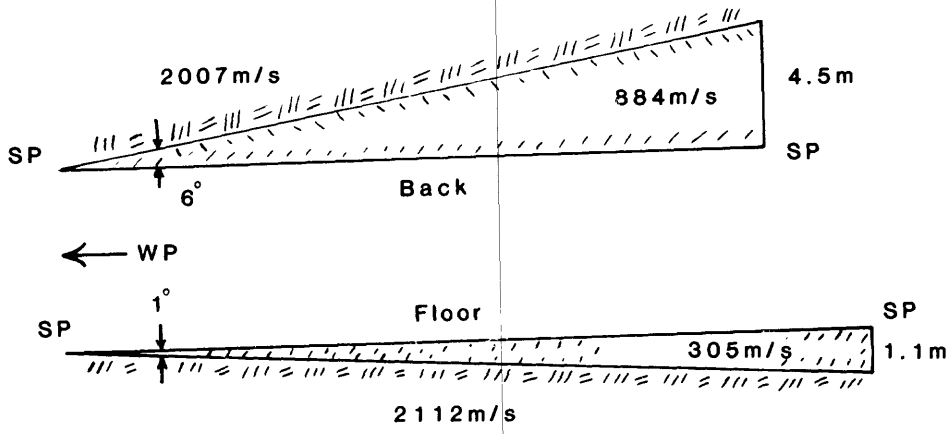

Figure 12.--Results of seismic survey in U12t.03 drift interpreted in terms of apparent dipping layer.

traveltime plot, or it is absent. Given the dips measured at locations encompassing our preshot refraction experience, the existence of the first premise would require velocity contrasts of 0.6 or less. A surface layer of such low velocity can be expected to be visually noteworthy on examination of the invert. This has not been our experience, and consequently, where the effects of dip may exist on the traveltime plot in preshot data we conclude a surface layer is either absent or its velocity is not significantly different from the average of the two-way velocities measured. Thus the enhancement of "dip" effects by ground shock seen on the t.03 data may be a diagnostic postshot parameter.

The U12t.04 Reentry

The t.04 reentry drift was freshly mined immediately following the Midas Myth event in order to examine the containment hardware of the experiment. No open drift existed at this location at the time of ground shock passage. In addition, the area is also free of geologic structure of the intensity mapped in the Ball Room. The results of the refraction survey at this location indicate that the velocities obtained are not separable from what one would expect in a preshot environment (fig. 10). The roof velocity (2637 m/s) is somewhat greater than that in the floor (2443 m/s); however, we ascribe no particular significance to this other than normal geologic variability. The offset in the traveltime segment in the floor suggesting faulting is occasionally seen in refraction surveys in the tunnels (Carroll and Kibler, 1983). It is observed near faults or where bedding plane contacts cross the geophone line. We believe it represents an interaction of the seismic wave and the bedding which manifests itself when the effects of dip or faulting raise a particular bed above the geophone line in the invert.

The Ball Room

Measurements were only attempted in the back of the Ball Room because the floor had been covered with a layer of concrete prior to the Midas Myth detonation. The floor of the Ball Room had moved upward along the fault near hole 7 (fig. 3) as a consequence of ground shock, and the back of the room was intensely fractured at many locations behind the wire mesh and shotcrete support. Because of the shotcrete, it was not possible to unequivocally locate where the tuff had not appreciably fractured, and the geophones were located in holes drilled in the firmest apparent locations in the back. At some locations it was apparent that firm rock was greater than a meter deep. The results of the survey in the Ball Room (fig. 11) indicate that the depth of fracturing was sufficient to yield significant delays in the arrival times. Another indication of significant deterioration in the coupling was the attenuation of arrivals in one direction to the extent they could not be reliably determined. The recourse of utilizing more energy in this situation was not available because of the hazard of shooting in the back. The results suggest the presence of pronounced "dip" effects similar to the t.03 data. The absence of agreement in the total two-way times negates any quantitative deductions from the data. Neither of the deeper velocities is representative of undisturbed tuff velocity. The 1480 m/s average of the two-way velocities is in agreement with the crosshole velocities obtained at depth in the holes in the back discussed in the next section.

MEASUREMENTS IN DRILL HOLES

As part of the evaluation of the damage resulting from the Midas Myth event, several holes were drilled for core testing and borescope examination in the vicinity of the Ball Room. Fourteen of the holes drilled 12 m in the floor and back were utilized for crosshole and inhole velocity measurements. The location of these holes in the floor (numbered 1 through 7) are shown on figure 3. The holes drilled in the back are at essentially the same locations. These holes have been renumbered for convenience of description from the official designations used by DNA. It should be noted that standing water occurred in all the holes in the floor at depths of 1.2 to 2.0 m (elevation 1604 m).

Measurements of inhole velocity were desired in two directions, along the length of the holes (perpendicular to the tunnel opening) and between holes (parallel to the tunnel opening). Experience in tuff in the perpendicular direction is limited, but similar measurements in granite suggest that it is reasonable to expect a zone of relief exhibiting a lower velocity near the tunnel opening (Carroll and others, 1966). Thus, the definition of this zone requires velocity sampling in the drill holes on sufficiently discrete intervals to define any anticipated low-velocity layer. This in turn requires, as in crosshole measurements, careful consideration to the interaction of the frequency of the source, the attenuation, characteristics of the medium, the frequency characteristics of the receivers, and the timing resolution of the recording system. Assuming a virgin-tuff velocity of about 2600 m/s (0.4 millisec/m) and the fact that fractured media are highly attenuating, these considerations become critical. It was considered possible that the fracturing in the tuff may degrade higher frequencies to the extent that only relatively low frequency energy might be detectable. This could result in only gross velocity data being obtained over two or three widely spaced inhole stations because of the inability to obtain good timing resolution. A similar concern applies to the spacing of holes for crosshole measurements.

The Velocity Probe

It was decided that the probe required for drill-hole measurements needed to be easily fabricated, disassembled, repaired, economically made, contain detectors of more than one orientation at each detector station, allow variable adjustments of the number and spacing of detectors, and be operable in drill holes at least 12 m deep at any orientation to the tunnel. Because the Ball Room was anticipated to be considerably fractured compared to preshot conditions, it was decided to utilize seismic caps as energy sources supplemented with a few centimeters of detonating cord where needed. This would yield the maximum energy and frequency spectrum commensurate with safety. In order to use minimum charge sizes, maximum sensitivity was required for the detectors. In addition, detectors were required that could be oriented in the standard three mutually perpendicular directions because of the desirability of recording shear waves. A final consideration was that the detectors be small enough to allow fabrication into a housing capable of insertion into a 7.6-cm-diameter drill hole.

Because of their small size, the L-21A geophones used in the refraction surveys in the back are ideally suited for such use; however, Mark Products

L-25D geophone inserts were finally selected because of their greater sensitivity. For smaller diameter probes or in an application requiring the necessity of installing a considerable number of stations on a probe, particularly in the vertically up mode, the use of an L21-A package might be more advantageous as it has about 1/3 the weight of the L-25D.

Measurement stations on the probe were made up in individual packages, 0.6 m in length. A minimum of three stations, each capable of housing three mutually perpendicular geophone units were constructed, with stations spaced a minimum of 1.5 m apart. The components and assembly are shown on figures 13-15. The geophone housing consisted of a solid block of PVC (diameter 5.1 cm) drilled with three mutually perpendicular holes in which the geophone packages were placed. This housing was inserted in 5.1-cm-ID Schedule 40 PVC and fastened with 10-31x3/16 set screws. The geophone packages were wired, waterproofed, and the electrical leads run inside the probe along a groove cut along one side of the housing. The geophone leads were 38 m in length and soldered at the ends to plug tips. These in turn were connected to a standard geophone cable utilizing the same 1.2 m leads described for the back surveys. The recording instrument was a Geometrics 1210F unit.

Each detector package was separated from the next station by 1.5-m lengths of 1.9-cm-diameter PVC tubing. The ends of the tubing were connected with roll pins or wire mesh placed in holes drilled in solid stock inserts seated inside the tubing with PVC weld. Thus, geophone stations could be separated by any multiple of 1.5 m desired. Between detector stations, the umbilicals for the electronic and air lines used to decentralize the probe were run outside these station spacers.

The geophones were decentralized against the walls of the drill holes by means of air-inflated rubber bladders fashioned from inner tubes and located at each end of the station packages. The individual bladders were fastened at each end around no. 7 rubber stoppers by means of hose clamps. The air line, consisting of 0.6-cm-diameter flexible tubing used to pressure the bladders, was run through holes in the ends of the rubber stoppers, passing through the inside of the geophone package via the same groove as the electrical leads. The pressure tubing at the ends of each geophone package was connected to a pressure fitting which in turn was connected to a similar fitting on the length of tubing used between individual stations. From the station nearest the hole collar, the tubing was run to a regulator and pressure gages via quick disconnects. Pressures from 138 to 276 kPa were used to decentralize the probe. The air-pressure line used in normal tunnel operations was used to provide the needed pressure.

The digital recorder was run on the 50-millisecond sweep range (sampling interval = 50 μsec). Frequencies on the order of 400-800 Hz were typically recorded at the deep detector stations. Occasionally, frequencies of 300 Hz were noted, presumably at those stations where fracturing was most intense.

Inhole Measurements

Inhole measurements were made in each hole with 2 detectors at each station, one oriented normal to the axis of the hole (parallel to the tunnel) and the other oriented parallel to the hole axis. For the inhole measurements, caps were successively detonated at the hole collars. Starting

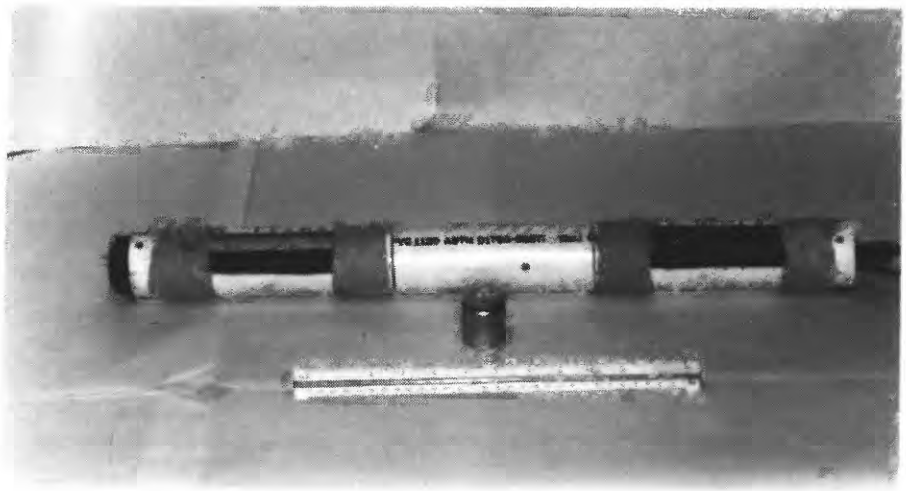

a)

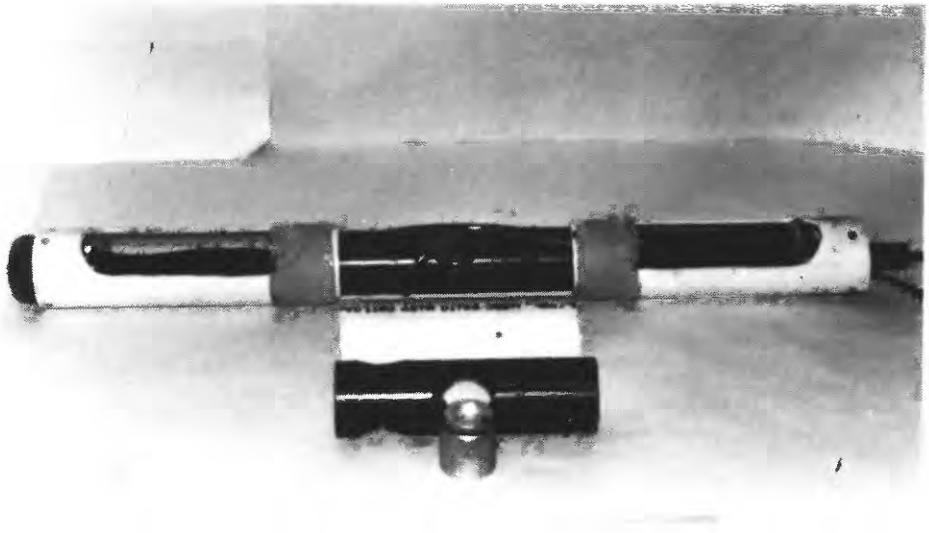

b)

Figure 13.--Details of geophone for velocity probe. a) Assembled package ready to go in hole. L-25D sensor also shown. b) Open package showing S-wave oriented detector wired in housing. Detector housing and sensor shown in foreground.

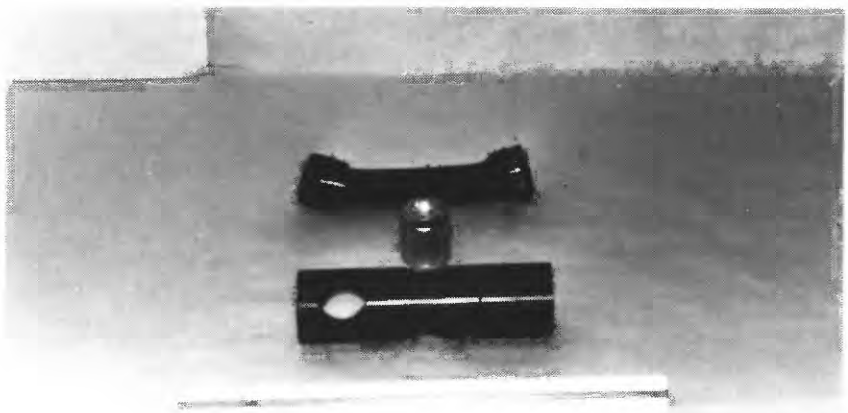

Figure 14.--Assembled air pressure bladder, L-25D geophone insert, and geophone housing block.

a)

b)

Figure 15.--a) Assembled velocity probe. b) Probe being inserted in hole 1 in back of Ball Room.

at the bottom of the hole, each measurement station consisted of three pairs of detectors on 1.5-m centers. Stations were successively occupied at 3-m intervals (one station overlap) coming out of the hole. The results of these measurements are shown on figure 16. Only the compressional velocity is depicted because it was seldom that an event that could be identified as the shear mode was seen on the transverse geophone. Whether this was the nature of the energy source, the nature of the media, or the nature of the detector mounts is not known. An example of a recording in which the shear wave was recorded is shown on figure 17. Our observations during these measurements suggest a considerable amount of experimentation would be required to generate the shear wave in this environment. Fortunately, the theory relating velocity change with fracturing indicates that for the purposes of this investigation the most diagnostic information is found in the behavior of the compressional velocity. However, it would have been useful to further examine the applicability of the theory in this environment by observing shear-wave behavior.

After the initial measurements from the holes in the back were reduced, the abnormally low velocities became of concern with regard to the accuracy of the data. Although we have no data base with respect to velocity measurements perpendicular to the tunnel in a room the size of the Ball Room, the velocities recorded are in general significantly outside the range of compressional velocities measured in the area preshot (fig. 4). This is also true when the data are compared to the preshot refraction velocity experience at all tunnel sites. In order to convince ourselves that probe spacing or design were not at fault, we measured the velocity in a steel pipe with the probe at the 1.5-m spacings used in the inhole surveys. We were able to accurately measure the steel velocity. As a further check for possible errors in timing resolution because of the short spacings used, we went back in the holes with the probe stations on larger (generally 4.6 m) spacings and again recorded the velocity. This procedure of making measurements on two different station spacings was continued in all of the holes. The results of the longer spacing surveys are also shown on figure 16. There is no significant difference except for hole 5 in the floor and hole 7 in the back. The long spacing velocities in the former were erroneously obtained with the bladders deflated, and coupling delays were created through the fluid in the hole resulting in low apparent velocities. The results in hole 7 are in agreement with regard to velocity, however, we have no explanation for the faster apparent arrivals in the small spacing data near the collar. Possibly some local dip, coupling phenomenon, or other error in the measurement is involved. As a final verification of the accuracy of the measurements obtained on 1.5-m spacings, repeat measurements made a day apart in hole 6 in the back are shown on figure 16. As a result of differences observed between the several surveys, we estimate the accuracy of the results to be generally within 10 percent.

Holes 3, 4, and 6 in the floor were all blocked at the time of the initial survey and had to be redrilled. They again caved, and 3 and 4 were eventually opened with a bar and line. Hole 3 was then surveyed with the long offset probe which was almost lost coming out of the hole. Rather than risk losing the probe no further attempts were made to insert the probe in either vertical holes 3 or 4. Velocity data were obtained in these three holes only in the long offset configuration and only to the depth of the caved sections in holes 4 and 6. (Holes 3 and 4 were sufficiently open to subsequently allow

page 31 follows

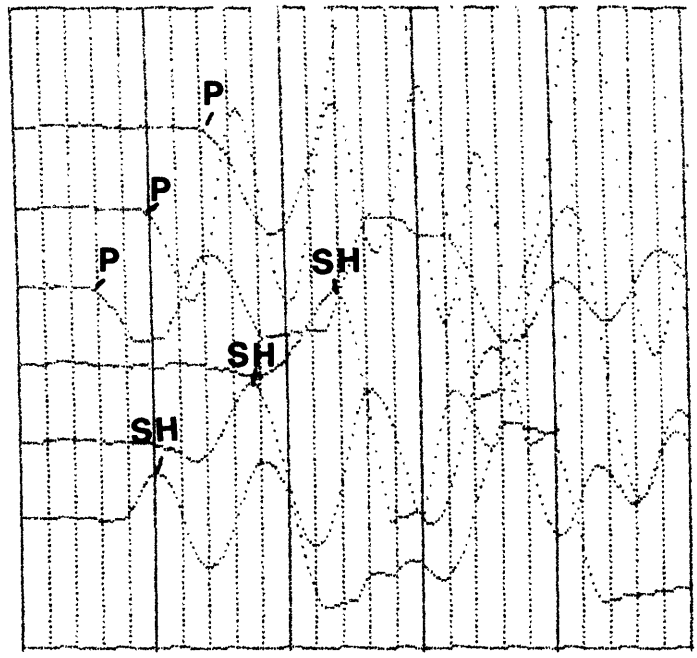

Figure 17.--Seismic record from Hole 4 in back illustrating P and SH arrivals. Detector spacing is 1.5 m, deepest station is 4.2 m in hole. Timing lines at 0.5 millisecond intervals.

their use as shotholes for the crosshole surveys.) It is doubtful if hole 6 can be maintained open without casing.

The results of the survey are depicted in bar graph form on figure 18. With the exception of the deeper portion of hole 1 in the back, the velocity of the rock in all the holes suggests varying degrees of fracturing subparallel to the tunnel, probably chiefly along bedding planes. The tuffs exhibiting the lowest velocity perpendicular to the drift are in hole 3 (floor) and hole 6 (floor and back). Both these holes are near the major faults mapped in the area. At the floor of the Ball Room, the fault in the vicinity of hole 6 is actually closer to hole 7. This fault moved under ground shock (fig. 19) and the absence of any appreciable velocity decrease in the tuff in the floor in hole 7, suggests major fracturing along the hanging wall. The induced movement along this fault was in the reverse mode which is often observed postshot elsewhere in the tunnels.

Another noteworthy feature is that the velocity in the back in hole 6 decreases with depth in the hole, a phenomenon peculiar to this hole. The foregoing suggest that the portion of the hanging wall near the fault plane may be the locus of maximum velocity damage induced by ground shock.

The presence of a lower velocity layer near the skin of the tunnel is found in several holes; however, the reduced velocities throughout the entire depth of most of the holes indicate that these data are generally only indicative of relatively greater fracturing near the tunnel skin. Undisturbed tuff velocity was never recorded in most of the holes. The presence of a fluid column in the holes in the floor apparently has little effect on the tuff velocity measured using the techniques applied in this experiment.

Crosshole Measurements

Crosshole velocity data were obtained in the back and floor using two probes in individual holes and detonating caps and a few centimeter lengths of detonating cord in a third hole. The probes were configured in the same manner as for the short-spaced inhole surveys. In these surveys, as in the inhole measurements, shear velocities were rarely recorded. The shotholes for these surveys were holes 3 and 5 in the back and holes 3 and 4 in the floor (fig. 3). For each triad of holes, the deepest detector stations were referenced to the elevation of the charge in the shothole with the exception of the measurement closest to the collar, where the reference was the middle detector station. Thus, the depths in the three holes comprising a measurement set refer to the depth from the collar to the charge in the shothole. These elevations were maintained by levelling a string line across the Ball Room. The setup of probes in the floor in holes 5 and 7 is shown on figure 19. The results of these measurements are shown on figures 20 and 21. Measurements were not made between holes 3 and 2 in the back because a deeply spalled zone was present between these holes.

Unlike the inhole velocity data, there is a distinct separation in the crosshole velocity results with lower velocities occurring in the roof. As there are no reported significant geologic variations at these two locations to which the differences can be attributed, we conclude that the fractures in the back have drained, whereas in the floor they remain saturated. The data obtained in the floor (fig. 21) suggest the presence of a low velocity surface

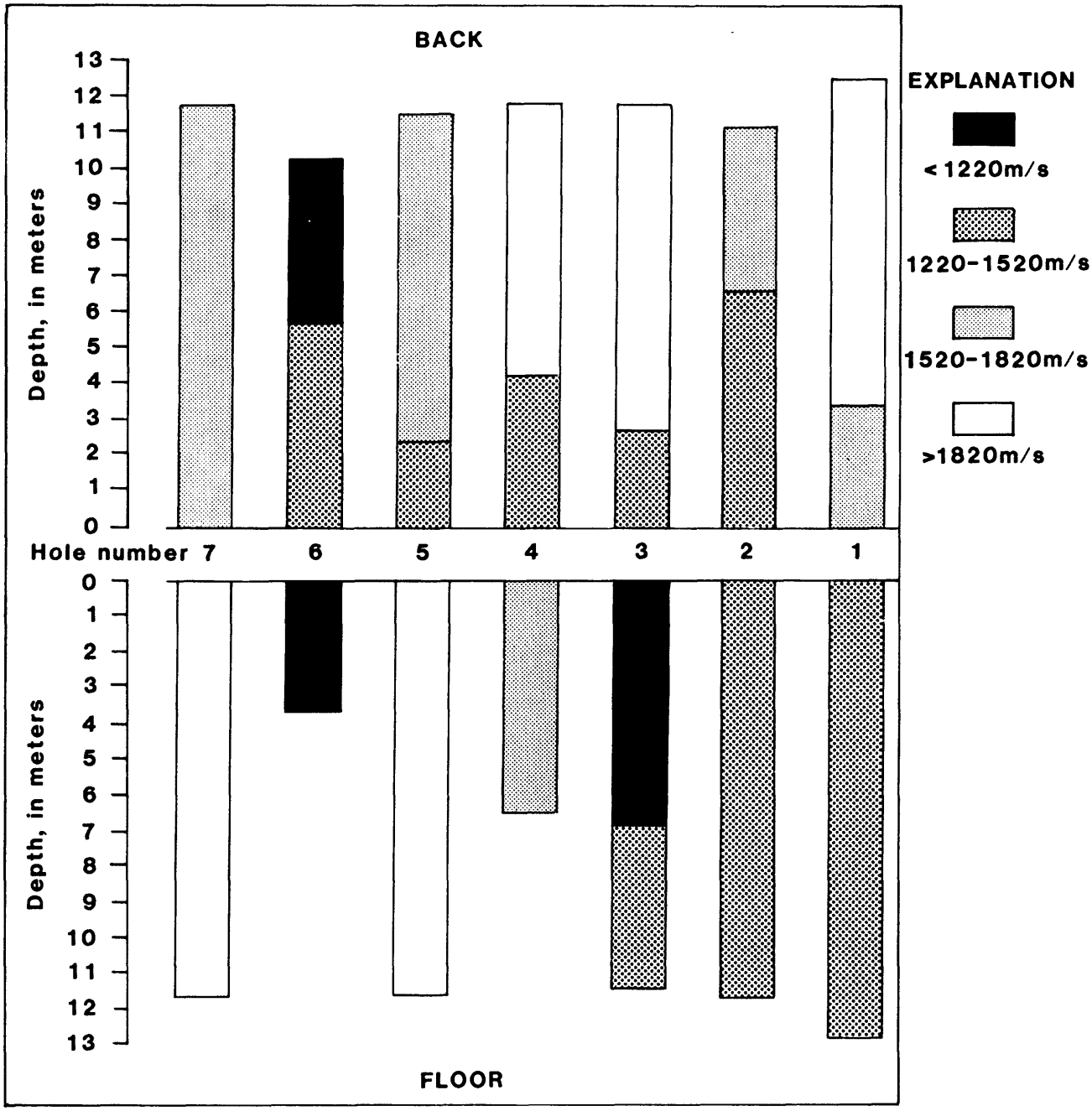

Figure 18.--Bar graph of results of inhole seismic velocities obtained in Ball Room.

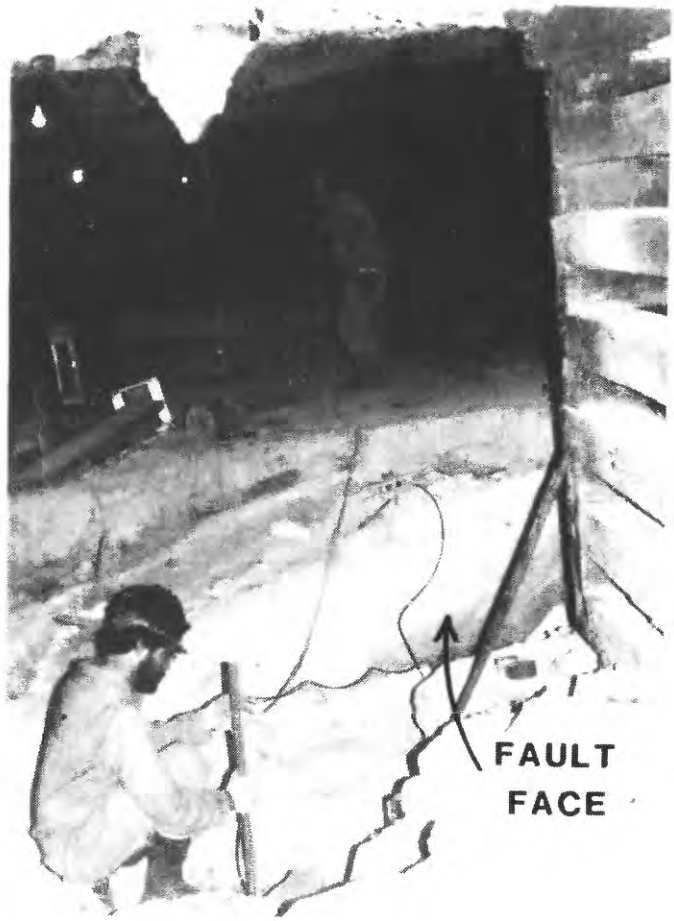

Figure 19.--Ball Room showing shock-induced offset along fault near hole 7. Fault face is exposed in foreground near cribbing. Offset in rear is a result of chipping out concrete. Personnel are seating probes in floor for crosshole survey between hole 7 (foreground) and hole 5 (rear).

page 31 follows

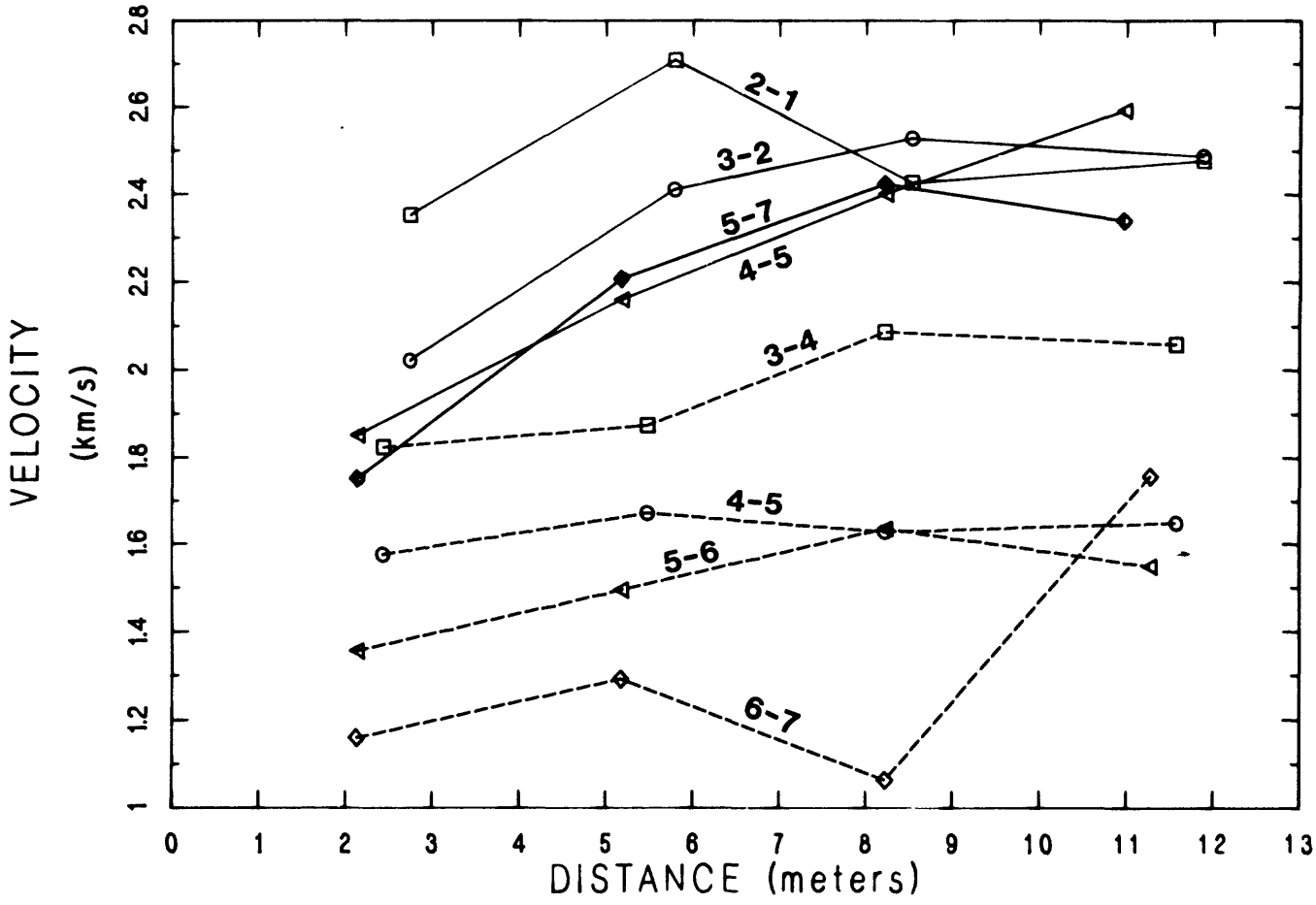

Figure 21.--Comparison of crosshole velocities obtained between holes in the floor (——) and back (---) of the Ball Room. Pairs of numbers indicate holes between which velocity was obtained as well as direction of travel of seismic wave.

layer near the hole collars. We believe this is the effect of the intensity and desaturation of fractures near the skin of the floor of the Ball Room.

SUMMARY OF DRILL-HOLE MEASUREMENTS

The drill-hole velocity measurements can best be summarized by comparison with the velocity experience obtained to date in unshocked environments. Figure 22 shows the results of such a comparison. The inhole data were thickness weighted by velocity and averaged. The crosshole data were obtained by a straight average of the velocities obtained at each level in the hole. The data representative of the undisturbed rock are the average of refraction velocities obtained in situ in 23 tunnels near the site of proposed nuclear detonations in tuff (Carroll and Kibler, 1983). The results of these comparisons indicate that the crosshole velocities in the floor of the Ball Room are comparable to velocities obtained in preshot tunnel environments, whereas the other inhole data are lower than normal. Since these velocity variations may fairly undisputedly be attributed to fractures, we note that the results of the theoretical variations of compressional velocity derived from Crampin's equations and plotted on figure 7 are not adequate to qualitatively explain our results because they treat a biplanar system of either totally wet or totally dry fractures. The inhole and crosshole data obtained in the back are adequately explained by the relationship presented on figure 7 if we consider both fracture systems to be dry. To qualitatively explain the variation in the data obtained in the floor in accordance with Crampin's theory, we need to examine an orthogonal set of fractures in which one set is dry, in this case the fracture (bedding plane) system in the floor subparallel to the drift, and the orthogonal set saturated, in this case the fractures (due to faulting) perpendicular to the Ball Room. This is done on figure 23, and the relative reduction in velocity as a function of orientation is listed in table 3. Our interest, of course, is for the orientation near 0° regardless of the measurement configuration (figs. 5c-5d) we are referencing. We note that the results of our measurements can be qualitatively explained by the theory.

Thus, standing water in the drill holes in the floor of the Ball Room may be concluded to be saturating the vertical fracture set. This set is sufficiently connected to have drained in the back. The fracturing or separation along planes of weakness that occurred subparallel to the tunnel as a result of ground shock passage may be concluded to represent an unconnected fracture system that is essentially dry in both the back and the floor of the Ball Room.

We recognize the possibility of an alternate explanation in that the fractures generated along the bedding could be of considerably greater density than those in the vertical. If so, then the general agreement of the magnitudes of the inhole velocities in the floor and back (fig. 22) suggests they have the same saturation state. The simplest explanation in light of the physical situation is that they are dry.

SUMMARY OF RESULTS

The refraction and drill-hole measurements both indicate that the tuffs in the vicinity of the Midas Myth experiment exhibit anomalously low velocity. Recorded compressional velocities are, in general, considerably

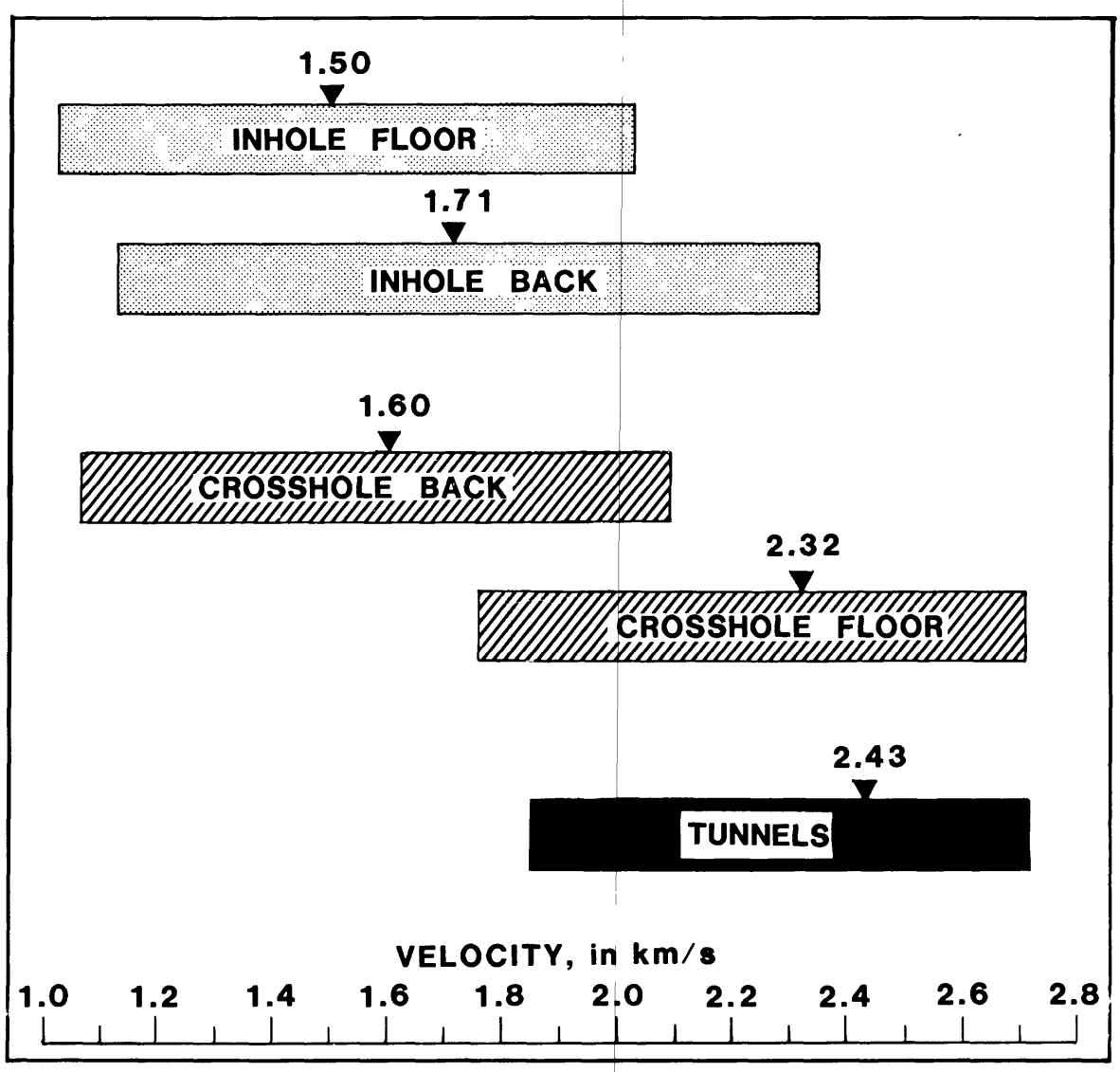

Figure 22.--Comparison of range and mean values of velocities obtained inhole and crosshole in the Ball Room with values obtained by refraction surveys in 23 tunnels in virgin tuff.

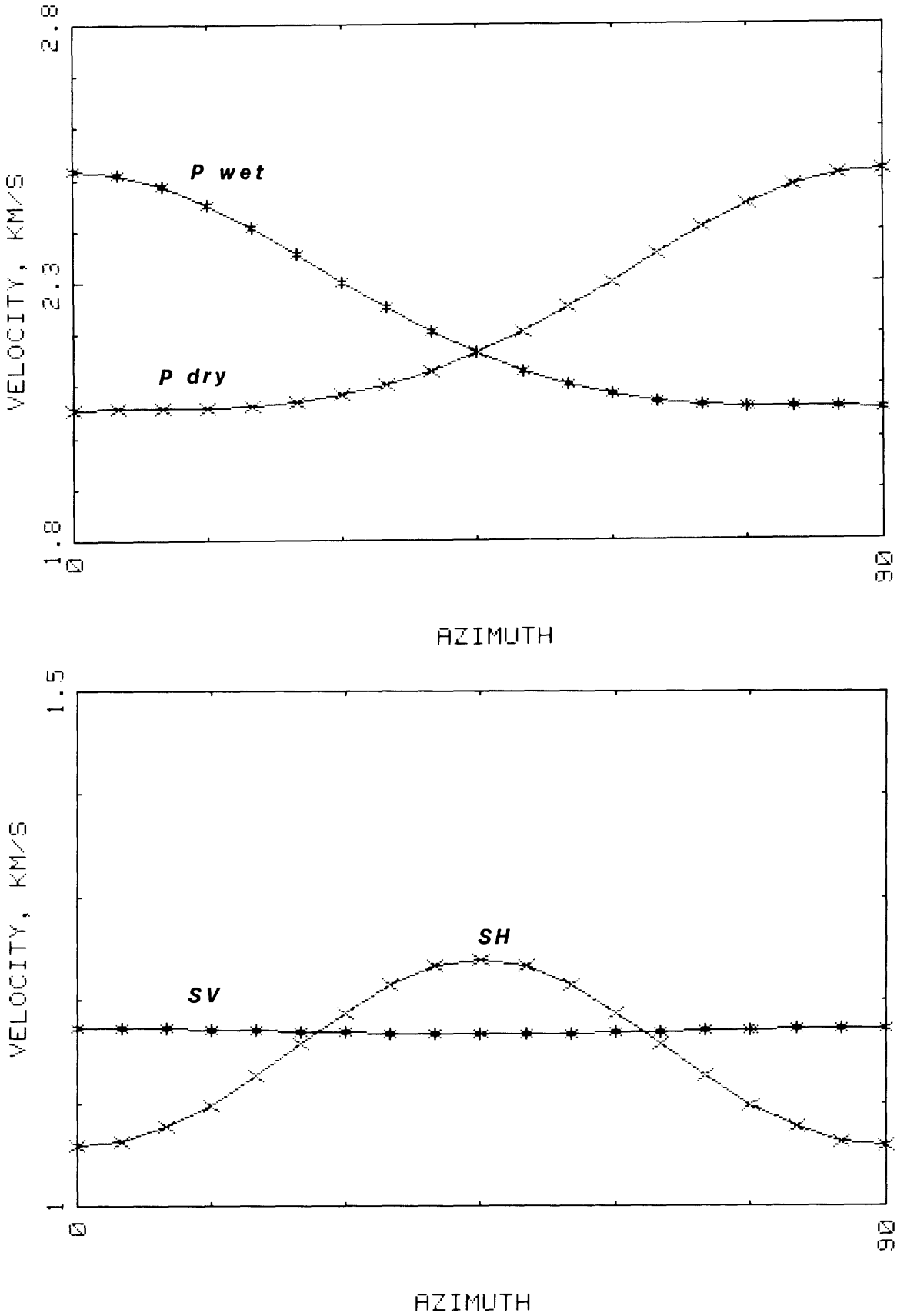

Figure 23.--Theoretical P- and S-wave velocities measured at various orientations for a biplanar (90°) set of fractures, one set of which is saturated and the other dry (* = wet set perpendicular to propagation direction at 0° which is case of crosshole configuration in the floor of the Ball Room; X = dry set perpendicular to propagation direction at 0° which is case of inhole configuration in the floor of Ball Room).

Table 3.--Normalized values of theoretical P- and S-wave velocity calculated for 5 degree azimuths to a biplanar (90 degree), wet- and dry-fracture system.

Azimuth	P		SH		SV
	(dry)	(wet)	(dry)	(wet)	(dry or wet)
0 [1]	0.791	0.968	0.814	0.814	0.902
5	0.791	0.965	0.818	0.818	0.902
10	0.791	0.956	0.828	0.828	0.902
15	0.791	0.942	0.845	0.845	0.901
20	0.793	0.925	0.866	0.866	0.900
25	0.796	0.905	0.890	0.890	0.899
30	0.801	0.885	0.914	0.914	0.899
35	0.809	0.866	0.935	0.935	0.898
40	0.819	0.848	0.949	0.949	0.898
45	0.832	0.832	0.953	0.953	0.897
50	0.848	0.819	0.949	0.949	0.898
55	0.866	0.809	0.935	0.935	0.898
60	0.885	0.801	0.914	0.914	0.899
65	0.905	0.796	0.890	0.890	0.899
70	0.925	0.793	0.866	0.866	0.900
75	0.942	0.791	0.845	0.845	0.901
80	0.956	0.791	0.828	0.828	0.902
85	0.965	0.791	0.818	0.818	0.902
90	0.968	0.791	0.814	0.814	0.902

[1] 0 degrees = Direction of wave propagation perpendicular to set described in headings.

below experience for undisturbed tuff, and in the Ball Room this condition exists for velocities perpendicular to the tunnel for the entire 12-m depth of most of the holes measured. This suggests that bedding plane detachment has been quite deep in the area as a result of ground shock. The crosshole data indicate a considerable reduction of velocity for energy travelling subparallel to the back as opposed to the floor of the Ball Room.

Refraction Surveys

Refraction surveys along the back of drifts appear to be a reasonable technique for monitoring velocity changes due to such things as drainage and tunnel relief with time. The utility of these measurements in areas subject to extensive ground-shock fracturing is subject to question. One should anchor detectors considerably deeper than was done in the Ball Room for the measurements reported here. A notable characteristic in the refraction data is the enhancement of "dip" effects in the postshot traveltime curve. Enhancement in this context means that the differences in two-way velocity (20 to 40 percent) greatly exceed the less than 10 percent differences observed in most preshot experience where such experience might be attributable to dip. Although the interpretation of a fractured, dipping layer best explains the data in the classical sense, we feel that these effects may actually be the result of a preferential fracturing direction or series of detachments near the tunnel skin presenting some as yet undetermined fracture model to yield the differences in two-way velocities. The lack of agreement in total two-way times noted in the refraction data obtained in the back of the Ball Room may in effect be reasonable in such a model. The two-way velocities obtained in these data suggest a preferential lower velocity in the direction away from the WP. This may not be fortuitous and requires further study. We have noted in connection with several unreported refraction investigations in freshly mined drifts near nuclear explosions that "dip" enhancement is often associated with the shear velocity close to the detonation point. A detailed examination of the relationship of this effect to dip or WP location has not been made.

Finally, we note that results of the refraction surveys in the t.04 reentry drift mined following the Midas Myth detonation yield velocities inseparable from undisturbed tuff velocity. This should not be surprising at the ranges from the detonation point we are dealing with here. Postshot velocity as a function of range from the detonation point has been discussed elsewhere (Carroll, 1983). With a few notable exceptions pre- and postshot measurements near underground openings as large as the Ball Room have not been recorded, and this geometry deserves further attention. Unfortunately no preshot refraction or drill-hole velocity data are available in the immediate area of the Ball Room.

Drill-Hole Surveys

The results of the drill-hole investigations confirm that a considerable difference in horizontal velocity exists in the Ball Room between the back and the floor. The higher velocity in the floor is attributed to the saturation of vertically connected fractures; these fractures having drained in the back. A second orthogonal set of fractures, unconnected and essentially dry, is concluded to have been enhanced and(or) created parallel to the Ball Room by the explosion, most reasonably by a detachment along bedding. The

compressional velocities obtained in the drill holes at various directions to these sets of fractures can be explained qualitatively by the relationships derived by Crampin concerning compressional velocity as a function of the orientation and saturation of biplanar fractures.

The data indicate greater velocity decreases near the skin of the Ball Room except for hole 6 in the back where velocity damage apparently has been greatest deeper in the hole. The data in this hole, when compared to hole 7 which is nearest the fault that moved under ground shock loading, and with the lower velocities near hole 3 also near a fault, suggest that maximum fracturing subparallel to the Ball Room occurred near these faults.

REFERENCES CITED

Carroll, R. D., 1983, Seismic velocity and postshot properties in and near chimneys, in Proceedings of the Monterey Containment Symposium, Monterey, Calif., August 26-28, 1981: Los Alamos National Laboratory Report LA-9211-C, p. 379-396.

Carroll, R. D., and Kibler, J. E., 1983, Sourcebook of locations of geophysical surveys in tunnels and horizontal holes including results of seismic refraction surveys, Rainier Mesa, Aqueduct Mesa, and Area 16, Nevada Test Site: U.S. Geological Survey Open-File Report 83-399, 85 p.

Carroll, R. D., Scott, J. H., and Cunningham, D. R., 1966, Uphole seismic measurements as an indication of stress relief in granitic rock tunnels: U.S. Geological Survey Professional Paper 550-D, p. D138-D143.

Crampin, Stuart, 1978, Seismic wave propagation through a cracked solid: Polarization as a possible dilatancy diagnostic: Geophysical Journal Royal Astronomical Society, v. 53, p. 467-496.

Crampin, S., McGonigle, R., and Bamford, D., 1980, Estimating crack parameters from observations of P-wave velocity anisotropy: Geophysics, v. 45, no. 3, p. 345-360.

Domenico, S. N., 1974, Effect of water saturation on seismic reflectivity of sand reservoirs encased in shale: Geophysics, v. 39, no. 6, p. 759-769.

_____1976, Effect of brine-gas mixture on velocity in an unconsolidated sand reservoir: Geophysics, v. 41, no. 5, p. 882-894.

Gibbons, A. B., Hinrichs, E. N., Hansen, W. R., and Lemke, R. W., 1963, Geology of the Rainier Mesa quadrangle, Nye County, Nevada: U.S. Geological Survey Geologic Quadrangle Map GQ-215, scale 1:24,000.

Leary, P. C., and Henyey, T. L., 1985, Anisotropy and fracture zones about a geothermal well from P-wave velocity profiles: Geophysics, v. 50, no. 1, p. 25-36.

O'Connell, R. J., and Budiansky, Bernard, 1974, Seismic velocities in dry and saturated cracked solids: Journal of Geophysical Research, v. 79, no. 35, p. 5412-5426.

Sargent, K. A., and Orkild, P. P., 1973, Geologic map of the Wheelbarrow Peak-Rainier Mesa Area, Nye County, Nevada: U.S. Geological Survey Miscellaneous Investigations Map I-754, scale 1:48,000.

U.S. GOVERNMENT PRINTING OFFICE: 1986—677-859 45,122 REGION NO. 8